

We thank the two reviewers for the detailed and thoughtful review of our manuscript entitled “Development and application of observable response indicators for design of an effective ozone and fine particle pollution control strategy in China”. Incorporation of the reviewers’ suggestion has led to a much improved manuscript. Detailed below is our response to the issues raised by the reviewers. We also detail the specific changes incorporated in the revised manuscript in response to the reviewers’ comments.

Reviewer #1:

[Comment]: *Identifying strategies that reduce the concentrations of secondary or mixed air pollutants most effectively is always a challenging work. This study partially answers this question by providing a new technique with combination of observation and RSM modeling indicators. Overall the paper is well written, I have minor comments for the authors to improve the paper and meet ACP requirements.*

[Response]: We thank the reviewer for recognition of the implications of the results of the analysis presented, and overall positive comments. We have followed all the comments and revised manuscript accordingly.

[Comment]: *The indicators are based on the chemical mechanisms and emissions in current models. Thus, the indicators may change for a different location or with improved mechanisms. I suggest authors add the limitations of this study in inclusion parts.*

[Response]: We agree with the reviewer that the indicators developed in this study were mainly based on the chemical mechanisms and emissions used in current study. They might change along with the improvement of scientific knowledge of chemical mechanisms. As the reviewer suggested, we point out such limitations in the revised manuscript, as follows.

(Page 22, Line 491-495) “We note that the discrepancy between the observable indicator and the responsive indicator might also be influenced by uncertainties in the chemical mechanism of CMAQ as well as prediction errors of the pf-RSM. The new indicators were designed based on the existing chemical mechanism, and the transition values might be refined in the future as our understanding of atmospheric chemical processes improves.”

[Comment]: *Only the title uses “particle” to represent particulate matter.*

[Response]: We thank the reviewer for noticing this issue. To address such problem and to be consistent through the text, we have modified the “fine particular matter” into “fine particle” when defining the PM<sub>2.5</sub> in the abstract and the introduction section, as follows.

(Page 1, Line 19-21) “Therefore, this study developed new observable RSM-based indicators and applied them to ambient fine particle (PM<sub>2.5</sub>) and ozone (O<sub>3</sub>) pollution control in China.”

(Page 3, Line 46-47) “In particular, ambient fine particles (PM<sub>2.5</sub>) and ozone (O<sub>3</sub>) are among the top risk factors for global mortality...”

[Comment]: *Clarifying some places and correcting grammar errors would help readers understand the paper better.*

[Response]: Followed the reviewer's suggestion, we corrected the grammar errors and did additional clarification in the revised manuscript.

[Comment]: *Lines 57-58, this sentence is not correct, for example, O<sub>3</sub> and NO<sub>x</sub> are correlated, but it is not due to the similarities in their atmospheric processes.*

[Response]: We agree with the reviewer that the original statement is a bit misleading. We have clarified it in the revised manuscript as follows.

(Page 3, Line 57-59) "Chemical species in the atmosphere are often highly correlated with one another, since their concentrations are affected by common atmospheric physical processes (e.g., mixing and transport) and chemical reactions."

[Comment]: *Line 58, not proper to call PM<sub>2.5</sub> as secondary pollutants.*

[Response]: We agree with the reviewer that the PM<sub>2.5</sub> can also come from primary emissions. To make the statement more accurate, we have deleted the secondary in the revised manuscript as follows.

(Page 3, Line 59-61) "Concentrations of pollutants such as O<sub>3</sub> and PM<sub>2.5</sub> are typically determined based on the ambient levels of their gaseous precursors, implying that O<sub>3</sub> and PM<sub>2.5</sub> chemistry can be identified through a combination of concentrations of some of their related chemical species (i.e., indicators)."

[Comment]: *Lines 106-108, this sentence does not belong here.*

[Response]: We agree with the reviewer that the original location of this sentence is inappropriate. We have moved it to the beginning of that paragraph in the revised manuscript, as follows.

(Page 5, Line 104-105) "The design of an effective O<sub>3</sub> and PM<sub>2.5</sub> control strategy requires efficient quantification of air pollutant sensitivity to precursor emissions."

Reviewer #2:

[Comment]: *The manuscript by Xing et al. on development and application of observable response indicators uses response surface modeling to identify parameters that define key O<sub>3</sub> and PM<sub>2.5</sub> production regimes, and then correlates these with observable indicators, i.e. ratios of gas and aerosol phase concentrations that are routinely measured. This provides valuable information that could be used to help design effective air quality policy to simultaneously reduce levels of both O<sub>3</sub> and PM<sub>2.5</sub> which, as the authors point out, has been a*

*challenge in China. The work is thus very relevant and suitable in scope for ACP. The paper is also very clearly written for the most part.*

[Response]: We thank the reviewer for recognition of the implications of the results of the analysis presented, and overall positive comments.

*[Comment]: My main comments are summarized as follows. The study currently neglect any errors in the polynomial approximations of the full CTM at later stages in the analysis, which I think is an oversight.*

[Response]: We agree with the reviewer on the importance of considering the error of polynomial approximations of the CTM. In the development of pf-RSM, we have examined the performance of pf-RSM to ensure its accuracy to meet the criteria of a mean normalized error within 2% and a maximal normalized error within 10%. The large errors are mostly located in the marginal areas where the emissions were reduced to nearly zero and the concentrations will be very small. Thus, the errors in the pf-RSM predictions have limited influence on the shape of nonlinear curve of the response function. To address the reviewer's concern, we have added following description about the error of pf-RSM in the revised manuscript.

(Page 8, Line 164-171) "The pf-RSM performance in predicting PM<sub>2.5</sub> and O<sub>3</sub> responses has been evaluated in detail using leave-one-out cross validation as well as the out-of-sample validation method, with normalized errors all within 5% for both PM<sub>2.5</sub> and O<sub>3</sub> across the domain. Relatively large biases occurred for marginal cases, where emissions are controlled by nearly 100% and predicted concentrations are very small. These cases have limited influence on the shape of nonlinear curve of the response function. However, the RSM is developed from a suite of CMAQ simulations, and so uncertainties in the chemical mechanism used in CMAQ might influence the O<sub>3</sub> and PM<sub>2.5</sub> predictions."

*[Comment]: Further, it is not mentioned explicitly that responses being analyzed here are with respect to domain wide emissions perturbations (I suspect, as it isn't explained clearly). This limits the applicability of these responses for evaluation of regional air quality control strategies, as there would be errors in using these relationships to estimate a response to a regional change in emissions.*

[Response]: We agree with the reviewer that the response of PM<sub>2.5</sub> and O<sub>3</sub> to different regional sources varies significantly. As suggested in our previous study (Xing et al., 2011), the local NO<sub>x</sub> controls can be either beneficial or unbeneficial in reducing O<sub>3</sub>, while regional NO<sub>x</sub> controls usually exhibit benefits in reducing O<sub>3</sub>. The overall effects are determined by the combination of the selected local/regional control ratios. In this study, the same level of emission perturbations was applied across the country. That is because controls are more likely taken in multiple regions of China rather than only on one single region. In addition, the same level of local and regional reduction is suggested to achieve aggressive air quality goals as demonstrated in our previous study (Xing et al., 2019).

To clarify this point, we have provided additional discussion in the revised manuscript, as follows.

(Page 7, Line 156-161) "Though the responses of O<sub>3</sub> and PM<sub>2.5</sub> to local or regional emissions vary significantly as suggested in our previous study (Xing et al., 2011), we applied the same change ratio of each pollutant emission to all regions across China. This approach is consistent with the implementation of a multi-regional joint control

strategy, which is reasonable for China. The same level of local and regional emission reduction has been recommended to achieve China's aggressive air quality goals (Xing et al., 2019)."

Reference:

Xing, J., Wang, S. X., Jang, C., Zhu, Y., and Hao, J. M.: Nonlinear response of ozone to precursor emission changes in China: a modeling study using response surface methodology, *Atmospheric Chemistry and Physics*, 11, 5027-5044, 10.5194/acp-11-5027-2011, 2011.

Xing, J., Zhang, F., Zhou, Y., Wang, S., Ding, D., Jang, C., Zhu, Y. and Hao, J.: Least-cost control strategy optimization for air quality attainment of Beijing–Tianjin–Hebei region in China. *Journal of environmental management*, 245, 95-104, 2019.

*[Comment]: Lastly, here are a few definitions / concepts that would be useful for the authors to define upfront (definitions of indicators that general audiences may not be familiar with).*

[Response]: As the reviewer suggested, we have defined the indicators including DSN, GR, and AdjGR, and provided references for PR and FR in the revised manuscript.

*[Comment]: Overall, the methods and results are interesting and have merit; all of these issues could be addressed with revisions to the text and some additional work on error analysis.*

[Response]: We have followed the reviewer's suggestion and made modification correspondingly in the text. Hope the revised manuscript can meet the high standard for ACP journal.

*[Comment]: 69: Please define DSN, GR, and AdjGR. Eventually I see later (line 233) that these are defined in the SI, but it would be more useful if they were defined earlier, or at least reference to where their definition can be found provided earlier.*

[Response]: As the reviewer suggested, we provide the definition of three indicators at the first time in the text, as follows.

(Page 4 Line 72-75) "Regarding PM<sub>2.5</sub> chemistry (more specifically for inorganic PM<sub>2.5</sub> sensitivities to NH<sub>3</sub> and NO<sub>x</sub>), indicators such as the degree of sulfate neutralization (DSN), gas ratio (GR), and adjusted gas ratio (AdjGR) have been developed (defined in Text S1) to identify NH<sub>3</sub>-poor or -rich conditions (Ansari and Pandis, 1998; Takahama et al., 2004; Pinder et al., 2008; Dennis et al., 2008)."

*[Comment]: 71: Clarify that by "these" you are referring to indicators for O3. I don't believe this has been done for the SIA indicators such as AdjGR since total nitrate isn't routinely observable from space.*

[Response]: We agree with the reviewer that “these” is referring to O<sub>3</sub> indicator. As the reviewer suggested, we have clarified it in the revised manuscript and moved this sentence ahead of the PM chemistry indicator, as follows.

(Page 4 Line 68-72) “The O<sub>3</sub> indicators can be derived from surface-monitoring observations (Peng et al., 2006), modeling simulations (Wang et al., 2010), or even satellite retrievals (Jin et al., 2017; Sun et al., 2018), and then examined using three-dimensional chemical transport models (CTMs) (Jiménez et al., 2004; Zhang et al., 2009; Liu et al., 2010; Ye et al., 2016).”

[Comment]: 85: Please define PR and FR..

[Response]: The PR and FR have been defined in our previous study (Xing et al., 2018). As the reviewer suggested, we provide the reference to clarify the definition of PR and FR in the revised manuscript, as follows.

(Page 4 Line 85-87) “Based on the RSM, the chemical response indicators of Peak Ratio (PR) and Flex Ratio (FR) have been designed to identify regimes of O<sub>3</sub> and PM<sub>2.5</sub> chemistry, respectively (see Xing et al., 2018 for detailed description of PR and FR).”

Reference:

Xing, J., Ding, D., Wang, S., Zhao, B., Jang, C., Wu, W., Zhang, F., Zhu, Y., and Hao, J. Quantification of the enhanced effectiveness of NO<sub>x</sub> control from simultaneous reductions of VOC and NH<sub>3</sub> for reducing air pollution in the Beijing–Tianjin–Hebei region, China, *Atmos. Chem. Phys.*, 18, 7799-7814, <https://doi.org/10.5194/acp-18-7799-2018>, 2018.

[Comment]: 101: What is meant by severe here? Are the goals to address severe episodes in the winter or address longer-term annual averages? As the chemical mechanisms driving the former are not well known, yet, my guess is the focus of this article is on the latter, which should be clarified.

[Response]: We agree with the reviewer that our target focuses on reducing long-term annual averages. To clarify this point, we have changed the “severe pollution” to “air pollution” in the revised manuscript, as follows.

(Page 5 Line 101-103) “Notably, accurate quantification of the nonlinear responses of O<sub>3</sub> and PM<sub>2.5</sub> to their precursor emissions is critical and a prerequisite for effective mitigation of air pollution in China.”

[Comment]: 143 - 146: The cited works here are not published yet, so please provide a brief summary of the performance benchmarks and statistics.

[Response]: We have updated the two cited papers which have been recently published or sent for publication. As the reviewer suggested, we also summarized the performance statistics in the revised manuscript as follows.

(Page 7 Line 148-152) “The normalized mean biases of CMAQ in predicting PM<sub>2.5</sub> and O<sub>3</sub> are -16.4% and -12.5% compared with monitoring data obtained from the China National Environmental Monitoring Centre. The mean

fractional biases for PM<sub>2.5</sub> and O<sub>3</sub> prediction are -14.2% and -11.1%, respectively (within the benchmark of  $\pm 60\%$ ). The mean fractional errors for PM<sub>2.5</sub> and O<sub>3</sub> prediction are 21.6% and 17.0% respectively (within the benchmark of 75%).”

Ding, D., Xing, J., Wang, S., Liu, K. and Hao, J.: Estimated Contributions of Emissions Controls, Meteorological Factors, Population Growth, and Changes in Baseline Mortality to Reductions in Ambient PM 2.5 and PM 2.5-Related Mortality in China, 2013–2017. *Environmental health perspectives*, 127(6), 067009, 2019a.

Ding, D., Xing, J., Wang, S., Chang, X. and Hao, J.: Impacts of emissions and meteorological changes on China’s ozone pollution in the warm seasons of 2013 and 2017, *Front. Environ. Sci. Eng.* 2019, 13(5): 76, 2019b.

*[Comment]: 155 - 263: I have questions about the spatial dimension of the terms in these equations. The manuscripts says that Xi was fit for every grid cell. Does that mean that in each grid cell it was known from the CTM simulations how Conc responded to each of the precursor emission species perturbed specifically in that grid cell? Or is it how Conc response to emissions perturbed uniformly throughout the entire model domain? If the former, that seems like a prohibitively large number of model runs (number of grid cells x 40). In this case then the response is the national average response? If the latter, it seems like the applicability of these equations for policy application is hindered by transport, in that it is now known if the change in concentration is occurring owing to changes in emissions in that location or emissions several hundred km upwind. In essence, a map of the response is not equivalent to a map of where the emissions changes need to be to elicit that response, hence this precludes using this information for region-specific changes to precursor emissions. Unless there are policies that aim to uniformly reduce emissions (from all sectors) the same amount throughout the country, it is hard to envision the direct applicability of these relationships for policy. Thus I’m not sure of the value of the province-specific values like those shown in Fig 11– a PR in a particular province isn’t necessarily associated with changes to emissions in that province alone.*

*[Response]:* We thank for the reviewer for raising a critical issue about the spatial match of responding grid cell and controlling grid cell. As the reviewer mentioned, it requires a large number of model runs to identify the controls for each grid cell, which is impossible. Thus, in this study, we applied the same level of emission perturbations to all grid cells across the country. The Xi was still fit for every grid cell, while the control factors represent the emission controls for the whole country, instead of the individual grid cell or region. We agree with the reviewer that the response of PM<sub>2.5</sub> and O<sub>3</sub> to different regional sources varies significantly. As found in our previous study (Xing et al., 2011), the local NO<sub>x</sub> controls can have either benefit or dis-benefit in reducing O<sub>3</sub>, while regional NO<sub>x</sub> controls usually exhibit benefit in reducing O<sub>3</sub>. The overall effects are determined by the combination of the selected local/regional control ratios. However, in China, multi-regional joint controls are more likely conducted rather than only controls on a single region. Besides, our previous study also recommended to apply the same local to regional control level for all regions to achieve air quality attainment with the maximal cost-benefit optimization (Xing et al., 2019). The province-specific values shown in Fig 11 provide an estimate of nonlinear response under the uniform-control case, which suggests the additional action needed for each province to avoid potential risk even after considering the multi-regional controls.

To clarify this point, we have added more discussion in the revised manuscript, as follows.

(Page 7, Line 156-161) “Though the responses of O<sub>3</sub> and PM<sub>2.5</sub> to local or regional emissions vary significantly as suggested in our previous study (Xing et al., 2011), we applied the same change ratio of each pollutant emission

to all regions across China in this study. This approach is consistent with the implementation of a multi-regional joint control strategy, which is reasonable for China. The same level of local and regional emission reduction has been recommended to achieve China's aggressive air quality goals (Xing et al., 2019)."

(Page 22, Line 475-478) "Since the indicators are developed from simulations with spatially uniform emission controls across the country, they are especially useful for providing quick estimates of the potential benefits or risks from uniform controls. These estimates can also provide a basis to design more localized control strategies for particular regions."

#### Reference:

Xing, J., Wang, S. X., Jang, C., Zhu, Y., and Hao, J. M.: Nonlinear response of ozone to precursor emission changes in China: a modeling study using response surface methodology, *Atmospheric Chemistry and Physics*, 11, 5027-5044, 10.5194/acp-11-5027-2011, 2011.

Xing, J., Zhang, F., Zhou, Y., Wang, S., Ding, D., Jang, C., Zhu, Y. and Hao, J.: Least-cost control strategy optimization for air quality attainment of Beijing–Tianjin–Hebei region in China. *Journal of environmental management*, 245, 95-104, 2019.

[Comment]: Fig 3: Please include units. Also define the domain over which the emissions perturbations are being considered here.

[Response]: As the reviewer suggested, we have included units (" $\mu\text{g m}^{-3}$ " for  $\text{PM}_{2.5}$  and "ppb" for  $\text{O}_3$ ), and clarified the emissions perturbations in the caption of Figure 3, as follows.

"Isopleth of population-weighted  $\text{PM}_{2.5}$  and daytime  $\text{O}_3$  to precursor emission change in different months. (The x- and y- axes represent precursor emission rates with a baseline of 1, applied to all grid cells in China; background colors represent the population-weighted  $\text{PM}_{2.5}$  and daytime  $\text{O}_3$  concentrations in China, with units of  $\mu\text{g m}^{-3}$  for  $\text{PM}_{2.5}$  and ppb for  $\text{O}_3$ )"

[Comment]: 245: I understand why 0 is a lower limit, but why is 2 an upper limit? This seems to cut off a lot of points in April (Fig 5).

[Response]: We agree with the reviewer that more points will be available for regression if we set the upper limit to be larger than 2. In this study, we set the range of emission changes as 0 to 2 to be consistent with our previous studies in which the pf-RSM performance has been well examined. Also, enlarging the upper limit will increase the sampling space, which might also increase the number of cases used to fit the pf-RSM.

To clarify this point, we have added some discussion in the revised manuscript, as follows.

(Page 8 Line 162-164) "The control matrix is provided in Table S2. The range of emission changes is set as 0 to 2 to be consistent with our previous studies in which the pf-RSM performance has been well examined (Xing et al., 2011; Wang et al., 2011; Xing et al., 2018; Ding et al., 2019b)."

*[Comment]: General: If a metric like FR and AdjGR don't agree, the authors are placing the blame entirely on the observable indicator e.g. AdjGR. However, there is some degree of inaccuracy in FR, related to the extent to which the pf-RSM explains the concentration responses. The authors should thus begin the results section with a summary of the accuracy of Eq 1, particularly in terms of discussing the residuals of this functional fit and their magnitudes, showing plots of the change in concentration predicted by FR or PF vs the actual change in concentrations.*

*Next, the magnitude of these residuals should be taken account when considering figures like 4 and 5. I suspect that the distinction of the 4 quadrants in each panel of Figs 4 and 5 directly along the axis is too strict. Rather, corresponding to the magnitude of the residual error in (1), the comparison for Figs 4 and 5 should be to identify points that lie some distance away from the quadrant boundaries, as points near the boundaries could be impacted by the error FR or PF.*

*Further, it's not clear in the writeup if the change in concentration in Eq 1 is that from the RSM or the CTM – this should be clarified. If the former, then there's an additional source of error that needs to be stated and accounted for, which is the RSM itself.*

*Lastly, these sources of error should be kept in mind in the presentation of all of the results comparing observable indicator responses vs RMS responses, e.g., discussion of Figs 7, 9, 10, 12*

*[Response]: We agree with the reviewer that the disagreement between FR and AdjGR can be influenced from uncertainties in both indicators, and it is importance to consider the error of polynomial approximations of the CTM. In the development of pf-RSM, we have examined the performance of pf-RSM to ensure its accuracy to meet the criteria of a mean normalized error within 2% and a maximal normalized error within 10%, comparing against with CMAQ. As we studied the pattern of the residuals (errors), large errors are mostly located in the marginal areas where the emissions were reduced to nearly zero and the concentration will be very small. Thus, the errors in pf-RSM has limited impacts on the shape of nonlinear curve of the response function. However, the uncertainties in the chemical mechanism of CMAQ will also contribute to the bias of O<sub>3</sub>/PM-chemistry determination. As the reviewer suggested, we have clarified the potential errors existed in CMAQ/RSM, and focused on our discussion on the observable indicators, in the revised manuscript, as follows.*

*(Page 8 Line 163-170) "The pf-RSM performance in predicting PM<sub>2.5</sub> and O<sub>3</sub> responses has been evaluated in detail using leave-one-out cross validation as well as the out-of-sample validation method, with normalized errors all within 5% for both PM<sub>2.5</sub> and O<sub>3</sub> across the domain. Relatively large biases occurred for marginal cases, where emissions are controlled by nearly 100% and predicted concentrations are very small. These cases have limited influence on the shape of nonlinear curve of the response function. However, the RSM is developed from a suite of CMAQ simulations, and so uncertainties in the chemical mechanism used in CMAQ might influence the O<sub>3</sub> and PM<sub>2.5</sub> predictions."*

*(Page 22 Line 491-495) "We note that the discrepancy between the observable indicator and the responsive indicator might also be influenced by uncertainties in the chemical mechanism of CMAQ as well as prediction errors of the pf-RSM. The new indicators were designed based on the existing chemical mechanism, and the transition values might be refined in the future as our understanding of atmospheric chemical processes improves."*



[Comment]: 201: As defined as the ratio of VOCs to NO<sub>x</sub>, it seems rather circuitous to derive this equation only to show that it reduces to the ratio of the coefficients for the linear VOC and NO<sub>x</sub> terms (i.e. x5/x6).

[Response]: The ratio of VOCs to NO<sub>x</sub> (VNr) is designed as the level of simultaneous control of VOCs to prevent an increase in O<sub>3</sub> levels from the NO<sub>x</sub> controls when PR<1 (VOC-limited). Thus we defined the VNr equals the ΔE<sub>voc</sub>/ΔE<sub>nox</sub> which makes first derivative of the ΔConcO<sub>3</sub> to ΔE<sub>nox</sub> equal 0. In the polynomial function of O<sub>3</sub> response to emissions, the first derivative of the ΔConcO<sub>3</sub> to ΔE<sub>nox</sub> (ΔE<sub>so2</sub>, ΔE<sub>nh3</sub> are 0, while ΔVOC is r × ΔE<sub>nox</sub>) is written as follows.

$$5 * X_1 * \Delta E_{NOx}^4 + 4 * X_2 * \Delta E_{NOx}^3 + 3 * X_3 * \Delta E_{NOx}^2 + 2 * X_4 * \Delta E_{NOx} + X_5 + X_6 * r + 2 * X_7 * r^2 * \Delta E_{NOx}^5 + 3 * X_8 * r^3 * \Delta E_{NOx}^2 + 2 * X_9 * r * \Delta E_{NOx}^2 + 4 * X_{10} * r^3 * \Delta E_{NOx}^3 + 6 * X_{11} * r * \Delta E_{NOx}^5 + 3 * X_{12} * r * \Delta E_{NOx}^2 = 0$$

Considering the NO<sub>x</sub> controls will be taken from baseline and ΔE<sub>nox</sub> is close to 0, we ignore the terms of ΔE<sub>nox</sub> in the first derivative function above, then it can be written as follows,

$$X_5 + X_6 * r = 0$$

Therefore, the VNr reduces to the ratio of the coefficients for the linear VOC and NO<sub>x</sub> terms.

We agree with the reviewer that the original description about VNr calculation is a bit ambiguous. We have clarified it in the revised manuscript as follows.

(Page 10 Line 219-231) “This level is defined by the ratio of VOCs to NO<sub>x</sub> (i.e., VNr) corresponding to the PR and is calculated as follows:

$$VNr = r \left| \frac{\partial \Delta Conc_{O_3}}{\partial \Delta E_{NOx}} \right|_{=0} \quad \text{when } PR < 1, \quad r = \Delta E_{VOC} / \Delta E_{NOx} \quad (4)$$

where  $\frac{\partial \Delta Conc_{O_3}}{\partial \Delta E_{NOx}}$  is the first derivative of the ΔConcO<sub>3</sub> to ΔE<sub>NOx</sub>. When ΔE<sub>VOC</sub> = r × ΔE<sub>NOx</sub>, and ΔE<sub>SO2</sub> and ΔE<sub>NH3</sub> are 0,  $\frac{\partial \Delta Conc_{O_3}}{\partial \Delta E_{NOx}}$  can be written as follows:

$$5 * X_1 * \Delta E_{NOx}^4 + 4 * X_2 * \Delta E_{NOx}^3 + 3 * X_3 * \Delta E_{NOx}^2 + 2 * X_4 * \Delta E_{NOx} + X_5 + X_6 * r + 2 * X_7 * r^2 * \Delta E_{NOx}^5 + 3 * X_8 * r^3 * \Delta E_{NOx}^2 + 2 * X_9 * r * \Delta E_{NOx}^2 + 4 * X_{10} * r^3 * \Delta E_{NOx}^3 + 6 * X_{11} * r * \Delta E_{NOx}^5 + 3 * X_{12} * r * \Delta E_{NOx}^2 = 0 \quad (5)$$

Since the ΔE<sub>NOx</sub> is close to 0 when the controls are taken from the baseline, we ignore the terms of ΔE<sub>NOx</sub> in the first derivative function above, then it can be written as follows,

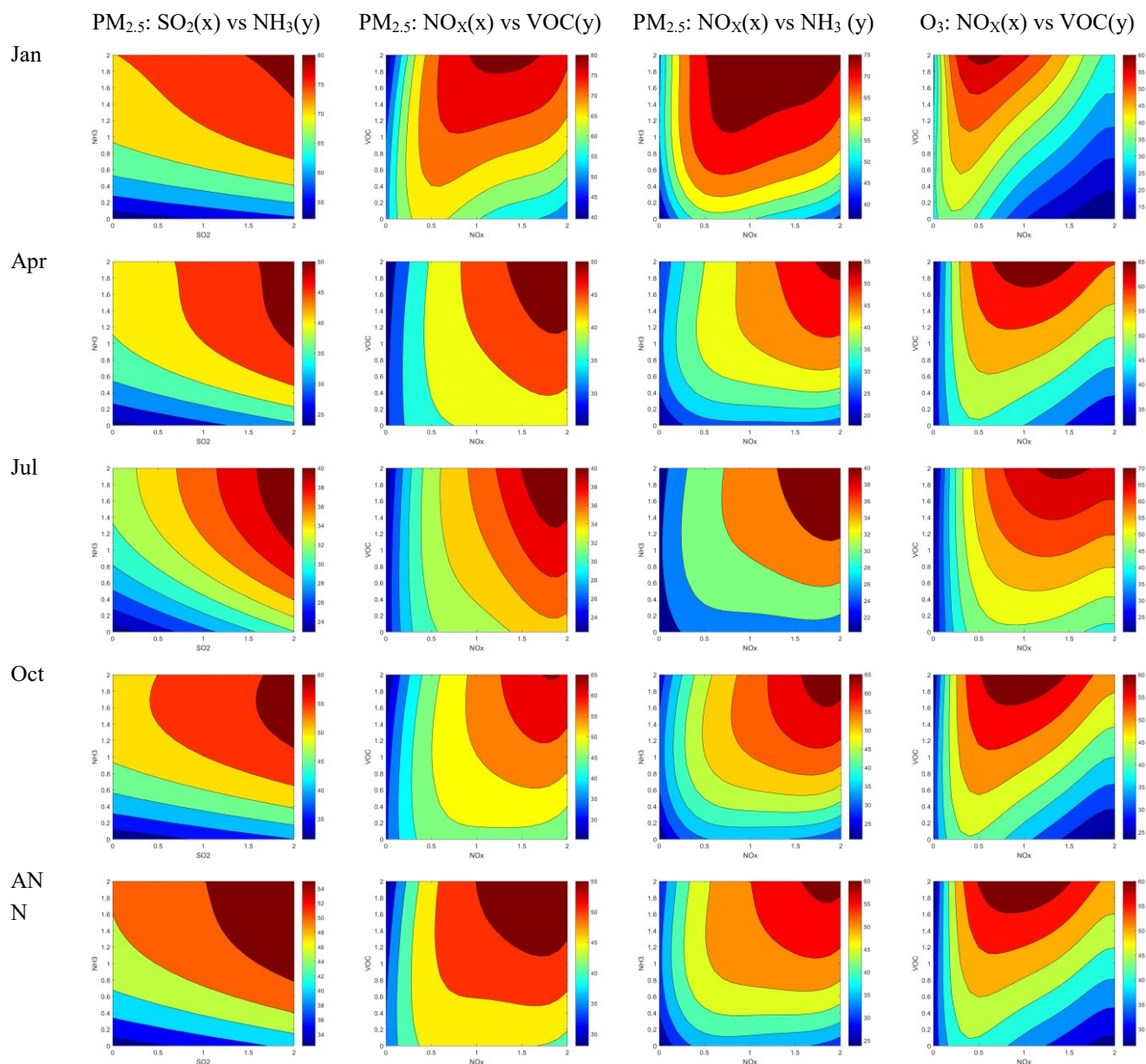
$$X_5 + X_6 * r = 0 \quad (6)$$

The VNr therefore can be calculated using the following equation:

$$VNr = - \frac{X_5}{X_6} \quad (7)''$$

[Comment]: 228: It is interesting that this change reduces down to just the linear response coefficient of PM2.5 with respect to NH3. This makes me want to see an additional plot in Fig 3 which is NH3 vs NO<sub>x</sub>.

[Response]: As the reviewer suggested, we have provided the PM<sub>2.5</sub> response to NH<sub>3</sub> and NO<sub>x</sub> in the Fig 3, as follows.



[Comment]: 275: Why is there a seasonal dependence to the performance of HCHO/NO<sub>2</sub>, particularly with such low performance in April?

[Response]: The seasonality of performance of the observable indicators (such as HCHO/NO<sub>2</sub>) in predicting O<sub>3</sub> chemistry might be associated with the uncertainty of the transition values, as different transition values were reported by different studies or for different location and time (Zhang et al., 2009). In this study, we found that

the performance of the HCHO/NO<sub>2</sub> can be substantially improved by using the transition value of 0.5 instead of 1, as shown in Table 2. Such result also implies that those indicators by using concentrations of just two species cannot fully consider all factors that determine the O<sub>3</sub> chemistry.

To clarify this point, we have added some discussion in the revised manuscript, as follows.

(Page 14 Line 301-305) “However, the performance of HCHO/NO<sub>y</sub> and HCHO/NO<sub>2</sub> could be greatly improved by using lower transition values, with increased annual success rates as high as 76 %. The change of the transition values implies that such indicators cannot fully consider all factors that determine the O<sub>3</sub> chemistry by using concentrations of just two species.”

#### Reference:

Zhang, Y., Wen, X. Y., Wang, K., Vijayaraghavan, K., and Jacobson, M. Z.: Probing into regional O<sub>3</sub> and particulate matter pollution in the United States: 2. An examination of formation mechanisms through a process analysis technique and sensitivity study, *Journal of Geophysical Research-Atmospheres*, 114, 31, 10.1029/2009jd011900, 2009.

*[Comment]: 384: Could the authors comment on the practicality of this application? I’m having a hard time imagining simultaneous equal %-based reductions to China-wide NH<sub>3</sub> and NO<sub>x</sub> emissions resulting from any real policy, given that these would be coming largely from different sectors, in different locations.*

*[Response]:* We understand the reviewer’s concern that the control strategy may not be uniform across the country, since it is impossible to require all regions to follow the same reduction rates, even though it might be cost-efficient for long term air quality attainment (Xing et al., 2019). However, the indicator-based approach, which uses the ambient concentrations of only a few species, can quickly estimate the potential benefit or risk from the uniform controls, which can act as a basis to design more localized control strategies for particular regions. For example, additional simultaneous VOC control with NO<sub>x</sub> is recommended in regions located at VOC-limited regime.

As the reviewer suggested, we have provided some discussion about the usage of indicator in the revised manuscript, as follows.

(Page 22 Line 476-479) “Since the indicators are developed from simulations with spatially uniform emission controls across the country, they are especially useful for providing quick estimates of the potential benefits or risks from uniform controls. These estimates can also provide a basis to design more localized control strategies for particular regions.”

#### Reference:

Xing, J., Zhang, F., Zhou, Y., Wang, S., Ding, D., Jang, C., Zhu, Y. and Hao, J.: Least-cost control strategy optimization for air quality attainment of Beijing–Tianjin–Hebei region in China. *Journal of environmental management*, 245, 95-104, 2019.

[Comment]: 420: What are the control pathways considered here? Ah  $\hat{A}$   $\hat{T}$  ok they are mentioned in the figure caption but it would be useful to add to the text.

[Response]: The control pathways considered here are six types of VOC-to-NO<sub>x</sub> control ratios, including 0, 0.2, 0.4, 0.6, 0.8 and 1.0. As the reviewer suggested, we have added such information in the revised manuscript as follows.

(Page 20 Line 445-447) “To explore the cobenefits of reducing O<sub>3</sub> and PM<sub>2.5</sub> after simultaneous control of NO<sub>x</sub> and VOCs, we investigated the effectiveness of six control pathways with various VOC-to-NO<sub>x</sub> ratios including 0, 0.2, 0.4, 0.6, 0.8 and 1.0 (Fig. 14).”

[Comment]: Fig 14: It's not clear to me how these results show that simultaneous reductions of O<sub>3</sub> and PM<sub>2.5</sub> are possible in January – as stated in the text. Rather, it looks like they are not except for all but one scenario (NO<sub>x</sub>:VOC = 1:1, only at the far end of the pathway). Potentially a very interesting figure here but it needs more explanation.

[Response]: Due to the strong NO<sub>x</sub>-saturated regime in January, compared to other months, a much larger VOC-to-NO<sub>x</sub> control ratio and greater NO<sub>x</sub> emission controls are required to prevent potential disbenefits from NO<sub>x</sub> controls and to achieve simultaneous reductions of O<sub>3</sub> and PM<sub>2.5</sub>. As demonstrated in Figure 14(a), there is only one pathway that can meet the simultaneous reductions of O<sub>3</sub> and PM<sub>2.5</sub> (i.e., that with VOC-to-NO<sub>x</sub> equal to 1 and at the far end of the pathway, with greater emission controls).

As the reviewer suggested, we have provided additional explanation about Figure 14 in the revised manuscript as follows.

(Page 20 Line 447-456) “In general, O<sub>3</sub> and PM<sub>2.5</sub> concentrations can be reduced in all months through simultaneous control of NO<sub>x</sub> and VOC emissions, although different VNr and control levels are required in different months. In January (under strongly NO<sub>x</sub>-saturated conditions), reductions in PM<sub>2.5</sub> and O<sub>3</sub> require VOC emission controls in addition to NO<sub>x</sub> controls to prevent potential disbenefits associated with the nonlinear chemistry. The smaller VNr required for PM<sub>2.5</sub> (~0.4) than for O<sub>3</sub> (~1.0) in this case might be associated with the smaller PR for PM<sub>2.5</sub> as well as the additional benefit of VOC controls in reducing secondary organic aerosols. Apparently, a larger VNr control ratio and greater emission control is required in January compared with other months. In Fig. 14(a), only one pathway can achieve simultaneous reduction in O<sub>3</sub> and PM<sub>2.5</sub> concentrations (i.e., the pathway with VNr equal to 1 and at the far end of the pathway, with reduction rates > 80%).”

[Comment]: 37: subscript on NO<sub>x</sub>.

[Response]: We have corrected it in the revised manuscript.

[Comment]: 51: Seinfeld et al. 2017 not in bibliography. Did the authors mean Seinfeld and Pandis (2012)?

[Response]: We are sorry for the typo. We have updated the reference to “Seinfeld and Pandis, 2012” in the revised manuscript.

[Comment]: 407 - 410: *There is perhaps a word missing or something from this sentence, please check.*

[Response]: As the reviewer suggested, we have revised this sentence in the revised manuscript as follows.

(Page 20 Line 433-436) “The PR results suggest strong NO<sub>x</sub>-saturated regimes in northern and eastern China including key regions such as the Sichuan Basin, YRD, and PRD, where simultaneous VOC control with a certain VOC-to-NO<sub>x</sub> ratio is required to prevent increases in O<sub>3</sub> levels from the NO<sub>x</sub> controls.”

# Development and application of observable response indicators for design of an effective ozone and fine particle pollution control strategy in China

Jia Xing<sup>1,2</sup>, Dian Ding<sup>1,2</sup>, Shuxiao Wang<sup>1,2,\*</sup>, Zhaoxin Dong<sup>1,2</sup>, James T. Kelly<sup>3</sup>, Carey Jang<sup>3</sup>, Yun Zhu<sup>4</sup>, Jiming Hao<sup>1,2</sup>

<sup>1</sup> State Key Joint Laboratory of Environmental Simulation and Pollution Control, School of Environment, Tsinghua University, Beijing 100084, China

<sup>2</sup> State Environmental Protection Key Laboratory of Sources and Control of Air Pollution Complex, Beijing 100084, China

<sup>3</sup> Office of Air Quality Planning and Standards, U.S. Environmental Protection Agency, Research Triangle Park, NC 27711, USA

<sup>4</sup> College of Environmental Science & Engineering, South China University of Technology, Guangzhou Higher Education Mega Center, Guangzhou, China

\*Corresponding Author: Shuxiao Wang (email: shxwang@tsinghua.edu.cn; phone: +86-10-62771466; fax: +86-10-62773650)

## Abstract

Designing effective control policies requires efficient quantification of the nonlinear response of air pollution to emissions. However, neither the current observable indicators nor the current indicators based on response-surface modeling (RSM) can fulfill this requirement. Therefore, this study developed new observable RSM-based indicators and applied them to ambient fine **particle** (PM<sub>2.5</sub>) and ozone (O<sub>3</sub>) pollution control in China. The performance of these observable indicators in predicting O<sub>3</sub> and PM<sub>2.5</sub> chemistry was compared with that of the current RSM-based indicators. H<sub>2</sub>O<sub>2</sub>×HCHO/NO<sub>2</sub> and total ammonia ratio, which exhibited the best performance among indicators, were proposed as new observable O<sub>3</sub>- and PM<sub>2.5</sub>-chemistry indicators, respectively. Strong correlations between RSM-based and traditional observable indicators suggested that a combination of ambient concentrations of certain chemical species can serve as an indicator to approximately quantify the response of O<sub>3</sub> and PM<sub>2.5</sub> to changes in precursor

emissions. The observable RSM-based indicator for O<sub>3</sub> (observable peak ratio) effectively captured the strong NO<sub>x</sub>-saturated regime in January and the NO<sub>x</sub>-limited regime in July, as well as the strong NO<sub>x</sub>-saturated regime in northern and eastern China and their key regions, including the Yangtze River Delta and Pearl River Delta. The observable RSM-based indicator for PM<sub>2.5</sub> (observable flex ratio) also captured strong NH<sub>3</sub>-poor condition in January and NH<sub>3</sub>-rich condition in April and July, as well as NH<sub>3</sub>-rich in northern and eastern China and the Sichuan Basin. Moreover, analysis of these newly developed observable response indicators suggested that the simultaneous control of NH<sub>3</sub> and NO<sub>x</sub> emissions produces greater benefits in provinces with higher PM<sub>2.5</sub> exposure by up to 12 µg m<sup>-3</sup> PM<sub>2.5</sub> per 10 % NH<sub>3</sub> reduction compared with NO<sub>x</sub> control only. Control of volatile organic compound (VOC) emissions by as much as 40 % of NO<sub>x</sub> controls is necessary to obtain the co-benefits of reducing both O<sub>3</sub> and PM<sub>2.5</sub> exposure at the national level when controlling NO<sub>x</sub> emissions. However, the VOC-to-NO<sub>x</sub> ratio required to maintain benefits varies significantly from 0 to 1.2 in different provinces, suggesting that a more localized control strategy should be designed for each province.

**Keywords:** nonlinear response, precursor emissions, response surface model, ozone, PM<sub>2.5</sub>, indicator

## 1. Introduction

Air pollution has attracted great attention because of its harmful effects on human health (Cohen et al., 2017), climate (Myhre et al., 2013), agriculture and ecosystems (Fuhrer et al., 2016), and visibility (Friedlander et al., 1977). In particular, ambient fine particles (PM<sub>2.5</sub>) and ozone (O<sub>3</sub>) are among the top risk factors for global mortality (Forouzanfar et al., 2015; Cohen et al., 2017) and have increased the need to effectively control anthropogenic sources in order to reduce the ambient concentrations of PM<sub>2.5</sub> and O<sub>3</sub> (Wang et al., 2017). The challenge is that the dominant contributions to ambient PM<sub>2.5</sub> and O<sub>3</sub> arise from a series of chemical reactions among precursors, including sulfur dioxide (SO<sub>2</sub>), nitrogen oxides (NO<sub>x</sub>), ammonia (NH<sub>3</sub>) and volatile organic compounds (VOCs) (Seinfeld and Pandis, 2012). The complexity of the chemical reactions and pathways associated with variations in meteorological conditions and precursor levels results in strong nonlinear responses of PM<sub>2.5</sub> and O<sub>3</sub> to their precursor emission changes (West et al., 1999; Hakami et al., 2004; Cohan et al., 2005; Pun et al., 2007; Megaritis et al., 2013). Such nonlinearity issues are a major challenge for policy-makers to design an effective control strategy.

Chemical species in the atmosphere are often highly correlated with one another, since their concentrations are affected by common atmospheric physical processes (e.g., mixing and transport) and chemical reactions. Concentrations of pollutants such as O<sub>3</sub> and PM<sub>2.5</sub> are typically determined based on the ambient levels of their gaseous precursors, implying that O<sub>3</sub> and PM<sub>2.5</sub> chemistry can be identified through a combination of concentrations of some of their related chemical species (i.e., indicators). The empirical kinetic modeling approach (EKMA) developed by the U.S. EPA quantifies the relationships of O<sub>3</sub> with its precursor concentrations based on O<sub>3</sub> chemistry (Freas et al., 1978; Gipson et al., 1981). The EKMA plot can aid inference of control strategy effectiveness (e.g., NO<sub>x</sub> or VOC control) according to VOC-to-NO<sub>x</sub> ratios. Several studies have developed “observable” indicators by relating O<sub>3</sub> to reactive



nitrogen concentrations and species related to atmospheric oxidation. Such indicators include  $\text{NO}_y$ ,  $\text{H}_2\text{O}_2/\text{HNO}_3$ ,  $\text{HCHO}/\text{NO}_2$  and  $\text{H}_2\text{O}_2/(\text{O}_3+\text{NO}_2)$  (Milford et al., 1994; Sillman, 1995; Tonnesen and Dennis, 2000; Sillman and He, 2002), which can be used to identify  $\text{NO}_x$ -saturated or -limited regimes. The  $\text{O}_3$  indicators can be derived from surface-monitoring observations (Peng et al., 2006), modeling simulations (Wang et al., 2010), or even satellite retrievals (Jin et al., 2017; Sun et al., 2018), and then examined using three-dimensional chemical transport models (CTMs) (Jiménez et al., 2004; Zhang et al., 2009; Liu et al., 2010; Ye et al., 2016). Regarding  $\text{PM}_{2.5}$  chemistry (more specifically for inorganic  $\text{PM}_{2.5}$  sensitivities to  $\text{NH}_3$  and  $\text{NO}_x$ ), indicators such as the degree of sulfate neutralization (DSN), gas ratio (GR), and adjusted gas ratio (AdjGR) have been developed (defined in Text S1) to identify  $\text{NH}_3$ -poor or -rich conditions (Ansari and Pandis, 1998; Takahama et al., 2004; Pinder et al., 2008; Dennis et al., 2008). The indicator-based method can be efficient in determining the chemical regime in the current scenarios and in qualitatively estimating  $\text{O}_3$  and  $\text{PM}_{2.5}$  sensitivities to small perturbations in precursor emissions or ambient concentrations without involving complex CTMs. However, traditional indicator methods are unable to quantify the extent of the chemistry regime (Pinder et al., 2008); hence, the traditional observable indicators provide policy-makers limited information for reducing  $\text{O}_3$  and  $\text{PM}_{2.5}$  pollution.

The sensitivity of  $\text{O}_3$  and  $\text{PM}_{2.5}$  to precursor emissions can be explored by running multiple brute-force CTM simulations. For instance, the response surface model (RSM) developed from brute-force simulations can generate a wide range of  $\text{O}_3$  and  $\text{PM}_{2.5}$  responses to precursor emissions ranging from fully controlled to doubled emissions (i.e., -100 % to 100 % change relative to the baseline emission) (Xing et al., 2011; Wang et al., 2011). Based on the RSM, the chemical response indicators of Peak Ratio (PR) and Flex Ratio (FR) have been designed to identify regimes of  $\text{O}_3$  and  $\text{PM}_{2.5}$  chemistry, respectively (see Xing et al., 2018 for detailed description of PR and FR). In contrast to the observable indicators, the PR and FR are meaningful values that represent the exact transition point at which a chemistry regime

89 converts to another regime. With the recent development of the polynomial function-based RSM (pf-  
90 RSM), the PR and FR can be easily calculated (Xing et al., 2018). However, this method is built on at  
91 least 20 CTM simulations; in other words, the estimating the PR and FR requires considerable computing  
92 resources. As a result, RSM use remains limited despite recent improvements in RSM efficiency (Xing et  
93 al., 2017).

94 Over the preceding decade, China's air quality has undergone substantial changes. In particular, the  
95 enactment of the *Air Pollution Prevention and Control Action Plan* from 2013 to 2017 greatly reduced  
96 PM<sub>2.5</sub> exposure (Zhao et al., 2018; Ding et al., 2019a). However, during this period, significant increases  
97 in O<sub>3</sub> concentrations were observed in most Chinese cities (Li et al., 2018). The rate of increase in O<sub>3</sub>  
98 concentration (based on the 90th percentile of daily maximum of 8-hr running average) was approximately  
99 27 %, 19 %, and 8 % in the North China Plain (NCP), Yangtze River Delta (YRD), and Pearl River Delta  
100 (PRD), respectively (Ding et al., 2019b). Greater control over anthropogenic sources must be enforced to  
101 reduce PM<sub>2.5</sub> and O<sub>3</sub> concentrations (Lu et al., 2018). Notably, accurate quantification of the nonlinear  
102 responses of O<sub>3</sub> and PM<sub>2.5</sub> to their precursor emissions is critical and a prerequisite for effective mitigation  
103 of air pollution in China.

104 The design of an effective O<sub>3</sub> and PM<sub>2.5</sub> control strategy requires efficient quantification of air  
105 pollutant sensitivity to precursor emissions. Indicator studies have demonstrated that the nonlinear  
106 response of O<sub>3</sub> and PM<sub>2.5</sub> to precursors can be estimated by using ambient concentrations of related  
107 chemical species. It is expected that the response indicators originally derived from RSM predictions (i.e.,  
108 PR and FR) can also be calculated using a combination of ambient concentrations of certain chemical  
109 species, enabling these indicators to become “observable” indicators rather than being dependent on  
110 numerous CTM simulations. To support the needs of policy design for O<sub>3</sub> and PM<sub>2.5</sub> control, this study  
111 developed effective indicators that not only represent O<sub>3</sub> and PM<sub>2.5</sub> chemistry but also aid in determining

the most feasible emission reduction path, similar to the benefits provided by RSM-based indicators. The flow of this study is presented in Fig. 1. The new observable response indicators were developed by investigating the link between observable and RSM-based indicators in China.

The remainder of this paper is structured as follows: Section 2 presents the detailed methods for CTM modeling, RSM configuration and response indicator development. Section 3 presents the evaluation of the performance of observable indicators in predicting the chemistry regime and the development of the observable response indicators and discusses their policy implications. Section 4 summarizes the main conclusions of this study.

## **2. Method**

### **2.1. Configuration of the CTM and RSM**

In this study, the Community Multi-scale Air Quality (CMAQ) model (version 5.2) was used to simulate the baseline concentrations of O<sub>3</sub> and PM<sub>2.5</sub> and their responses in numerous emission control scenarios with different emission change ratios. The simulation was conducted on a domain covering China with 27 km × 27 km horizontal resolution (Fig. 2). In 2017, January, April, July, and October were simulated to represent winter, spring, summer, and fall, respectively. An annual level was estimated as the average of the levels in these four months. The concentration data was analyzed based on the monthly average for afternoon O<sub>3</sub> (12:00–18:00 China Standard Time when O<sub>3</sub> was the highest across a day), and monthly average for 24-h PM<sub>2.5</sub>. To approximate exposure concentrations, we also estimated population-weighted O<sub>3</sub> and PM<sub>2.5</sub> at the regional or national level by averaging the gridded concentrations weighted by the population in each grid cell. The gridded population data were obtained from the 1 km × 1 km LandScan population dataset in 2016 (Oak Ridge National Laboratory, 2013).

The anthropogenic emission data were developed by Tsinghua University by using a bottom-up method (Ding et al., 2019a), with updated activity data from the 2017 China statistical yearbook as well

135 as the latest application rates of end-of-pipe control technologies based on the governmental bulletin and  
136 reports. The anthropogenic emissions were gridded into  $27\text{ km} \times 27\text{ km}$  horizontal resolution to match the  
137 CMAQ model (Fig. S1). The 2017 biogenic emissions over China were generated using the Model for  
138 Emissions of Gases and Aerosols from Nature (MEGAN; version 2.04). The meteorology field, driven by  
139 the Weather Research and Forecasting Model (WRF; version 3.7), followed the same configuration as that  
140 in our previous study (Ding et al., 2019a,b), and thus included the Morrison double-moment microphysics  
141 scheme, the RRTMG radiation scheme, Kain-Fritsch cumulus cloud parameterization, the Pleim-Xiu land-  
142 surface physics scheme, and the ACM2 PBL physics scheme. We used NCEP FNL (Final) Operational  
143 Global Analysis data for the initial and boundary conditions in the WRF. The comparison with observation  
144 data from the National Climatic Data Center suggested agreeable performance of the WRF model for  
145 simulating wind speed, humidity and temperature (Table S1). The CMAQ model performance in  
146 reproducing  $\text{O}_3$  and  $\text{PM}_{2.5}$  concentrations was evaluated by comparison with the ground-based  
147 observations (Fig. S2), which suggested acceptable CMAQ model performance that met the recommended  
148 benchmark (Ding et al., 2019a,b). The normalized mean biases of CMAQ in predicting  $\text{PM}_{2.5}$  and  $\text{O}_3$  are  
149 -16.4% and -12.5% compared with monitoring data obtained from the China National Environmental  
150 Monitoring Centre. The mean fractional biases for  $\text{PM}_{2.5}$  and  $\text{O}_3$  prediction are -14.2% and -11.1%,  
151 respectively (within the benchmark of  $\pm 60\%$ ). The mean fractional errors for  $\text{PM}_{2.5}$  and  $\text{O}_3$  prediction are  
152 21.6% and 17.0% respectively (within the benchmark of 75%). The RSM was developed based on multiple  
153 CTM simulations for various emission-control scenarios according to the brute-force method. Identical to  
154 our previous RSM studies (Xing et al., 2017, 2018), the responses of  $\text{O}_3$  and  $\text{PM}_{2.5}$  to precursor emissions  
155 were analyzed using the baseline case and 40 control scenarios using the Latin Hypercube Sample method  
156 for four control variables, namely the emission ratios of  $\text{NO}_x$ ,  $\text{SO}_2$ ,  $\text{NH}_3$ , and VOCs. Though the responses  
157 of  $\text{O}_3$  and  $\text{PM}_{2.5}$  to local or regional emissions vary significantly as suggested in our previous study (Xing

et al., 2011), we applied the same change ratio of each pollutant emission to all regions across China in this study. This approach is consistent with the implementation of a multi-regional joint control strategy, which is reasonable for China. The same level of local and regional emission reduction has been recommended to achieve China's aggressive air quality goals (Xing et al., 2019).

The control matrix is provided in Table S2. The range of emission changes is set as 0 to 2 to be consistent with our previous studies in which the pf-RSM performance has been well examined (Xing et al., 2011; Wang et al., 2011; Xing et al., 2018; Ding et al., 2019b). The pf-RSM performance in predicting PM<sub>2.5</sub> and O<sub>3</sub> responses has been evaluated in detail using leave-one-out cross validation as well as the out-of-sample validation method, with normalized errors all within 5% for both PM<sub>2.5</sub> and O<sub>3</sub> across the domain. Relatively large biases occurred for marginal cases, where emissions are controlled by nearly 100% and predicted concentrations are very small. These cases have limited influence on the shape of nonlinear curve of the response function. However, the RSM is developed from a suite of CMAQ simulations, and so uncertainties in the chemical mechanism used in CMAQ might influence the O<sub>3</sub> and PM<sub>2.5</sub> predictions.

## 2.2. RSM-based indicators of O<sub>3</sub> and PM<sub>2.5</sub> chemistry

Based on the developed pf-RSM, the nonlinear responses of O<sub>3</sub> and PM<sub>2.5</sub> concentrations to precursor emissions can be represented as follows:

$$\Delta Conc = \sum_{i=1}^n X_i \cdot (\Delta E_{NOx})^{a_i} \cdot (\Delta E_{SO2})^{b_i} \cdot (\Delta E_{NH3})^{c_i} \cdot (\Delta E_{VOCs})^{d_i} \quad (1)$$

where  $\Delta Conc$  is the change in O<sub>3</sub> or PM<sub>2.5</sub> concentration from the baseline concentration calculated from a polynomial function of four variables ( $\Delta E_{NOx}$ ,  $\Delta E_{SO2}$ ,  $\Delta E_{NH3}$ ,  $\Delta E_{VOCs}$ );  $\Delta E_{NOx}$ ,  $\Delta E_{SO2}$ ,  $\Delta E_{NH3}$ , and  $\Delta E_{VOCs}$  are the change ratios of NO<sub>x</sub>, SO<sub>2</sub>, NH<sub>3</sub>, and VOC emissions (i.e.,  $\Delta Emissions / Baseline\_Emissions$ ), respectively, relative to the baseline emissions (baseline = 0); and  $a_i$ ,  $b_i$ ,  $c_i$ , and  $d_i$  are the nonnegative integer powers of  $\Delta E_{NOx}$ ,  $\Delta E_{SO2}$ ,  $\Delta E_{NH3}$ , and  $\Delta E_{VOCs}$ , respectively.  $X_i$  is the coefficient of term  $i$  for the 14

181 ( $n$ ) terms listed in Table 1.

182 The terms used to represent PM<sub>2.5</sub> and O<sub>3</sub> responses were determined in designing the pf-RSM  
183 (Table 1). The high-degree terms of NO<sub>x</sub>, VOCs and NH<sub>3</sub> represent their strong nonlinear contributions to  
184 O<sub>3</sub> or PM<sub>2.5</sub>. The interaction terms of NO<sub>x</sub> and VOC for PM<sub>2.5</sub> and O<sub>3</sub> represent the nonlinearity in  
185 atmospheric oxidations, whereas those of NO<sub>x</sub> and NH<sub>3</sub> for PM<sub>2.5</sub> represent aerosol thermodynamics (Xing  
186 et al., 2018).

187  $X_i$  was fitted by 40 CTM control scenarios for each spatial grid cell. The  $X_i$  values in the pf-RSM  
188 for annual-averaged population-weighted O<sub>3</sub> and PM<sub>2.5</sub> concentrations in 31 provinces in China are  
189 provided in Table S3 and Table S4, respectively. The terms with first degree for NO<sub>x</sub>, SO<sub>2</sub>, NH<sub>3</sub>, and  
190 VOCs represent the first derivative of PM<sub>2.5</sub> and O<sub>3</sub> response to each precursor emission. O<sub>3</sub> was more  
191 sensitive to NO<sub>x</sub> (term  $X_5$ ) and VOCs (term  $X_6$ ) than to SO<sub>2</sub> (term  $X_{13}$ ) or NH<sub>3</sub> (term  $X_{14}$ ), and O<sub>3</sub>  
192 sensitivity was negative to NO<sub>x</sub> but positive to VOCs in most provinces. PM<sub>2.5</sub> sensitivities to the four  
193 precursors (terms  $X_1$ ,  $X_2$ ,  $X_5$  and  $X_{11}$  for VOCs, NH<sub>3</sub>, SO<sub>2</sub>, and NO<sub>x</sub>, respectively) were comparable,  
194 whereas PM<sub>2.5</sub> sensitivity to NO<sub>x</sub> could be negative or positive.

195 The nonlinearities of O<sub>3</sub> and PM<sub>2.5</sub> to precursors were mainly determined by high-order and  
196 interaction terms. To illustrate such nonlinearities further, we used a series of isopleths, as shown in Fig.  
197 3, as an example to present the national-averaged PM<sub>2.5</sub> response to SO<sub>2</sub> and NH<sub>3</sub>, NO<sub>x</sub> and NH<sub>3</sub>, as well  
198 as PM<sub>2.5</sub> and O<sub>3</sub> responses to NO<sub>x</sub> and VOCs in different months. Strong nonlinearity was noted in PM<sub>2.5</sub>  
199 sensitivity to NH<sub>3</sub>, and in O<sub>3</sub> and PM<sub>2.5</sub> sensitivities to NO<sub>x</sub>. PM<sub>2.5</sub> sensitivity to NH<sub>3</sub> increased alongside  
200 the transition of PM<sub>2.5</sub> chemistry from the NH<sub>3</sub>-rich condition (typically at high NH<sub>3</sub> emission ratios) to  
201 the NH<sub>3</sub>-poor condition (typically at low NH<sub>3</sub> emission ratios). O<sub>3</sub> and PM<sub>2.5</sub> sensitivities to NO<sub>x</sub> were  
202 negative under the NO<sub>x</sub>-saturated regime (typically at high NO<sub>x</sub> emission ratios) but became positive  
203 under the NO<sub>x</sub>-limited regime (typically at low NO<sub>x</sub> emission ratios). In addition, the transition points

(corresponding to the NO<sub>x</sub> or NH<sub>3</sub> ratios at which the chemical regime for O<sub>3</sub> or PM<sub>2.5</sub> chemistry changed) varied by time (Fig. 3) and space (see the isopleths at different provinces in Figs S3-S6). In general, the NH<sub>3</sub>-poor condition appears in winter because of low NH<sub>3</sub> evaporation and little agriculture activity which is a dominant NH<sub>3</sub> source. The strong NO<sub>x</sub>-saturated condition appears in winter when photolysis is less active than in other seasons, and concentrates in industrial regions with abundant NO<sub>x</sub> emissions.

To further quantify the aforementioned nonlinearity, two RSM-based response indicators (i.e., the PR for O<sub>3</sub> and FR for PM<sub>2.5</sub>) were calculated as described in our previous studies (Xing et al., 2011, 2018; Wang et al., 2011).

For O<sub>3</sub>, the PR can be directly calculated as follows:

$$PR = 1 + \Delta E_{NOx} \Big|_{\frac{\partial \Delta Conc_{O_3}}{\partial \Delta E_{NOx}}=0} E_{NOx} \in [a, b] \quad (2)$$

where  $\frac{\partial \Delta Conc_{O_3}}{\partial \Delta E_{NOx}}$  is the first derivative of the  $\Delta Conc_{O_3}$  to  $\Delta E_{NOx}$ , which can be derived as follows:

$$5 * X_1 * \Delta E_{NOx}^4 + 4 * X_2 * \Delta E_{NOx}^3 + 3 * X_3 * \Delta E_{NOx}^2 + 2 * X_4 * \Delta E_{NOx} + X_5 = 0 \quad (3)$$

The PR is the NO<sub>x</sub> emissions (represented as  $1 + \Delta E_{NOx}$ ) that produce maximum O<sub>3</sub> concentration under the baseline VOC emissions. For  $PR < 1$ , the baseline condition is NO<sub>x</sub> saturated, and the level of simultaneous control of VOCs to prevent an increase in O<sub>3</sub> levels from the NO<sub>x</sub> controls must be understood. This level is defined by the ratio of VOCs to NO<sub>x</sub> (i.e., VNr) corresponding to the PR and is calculated as follows:

$$VNr = r \Big|_{\frac{\partial \Delta Conc_{O_3}}{\partial \Delta E_{NOx}}=0} \text{ when } PR < 1, r = \Delta E_{VOC} / \Delta E_{NOx} \quad (4)$$

where  $\frac{\partial \Delta Conc_{O_3}}{\partial \Delta E_{NOx}}$  is the first derivative of the  $\Delta Conc_{O_3}$  to  $\Delta E_{NOx}$ . When  $\Delta E_{VOC} = r \times \Delta E_{NOx}$ , and  $\Delta E_{SO_2}$  and  $\Delta E_{NH_3}$  are 0,  $\frac{\partial \Delta Conc_{O_3}}{\partial \Delta E_{NOx}}$  can be written as follows:

$$5 * X_1 * \Delta E_{NOx}^4 + 4 * X_2 * \Delta E_{NOx}^3 + 3 * X_3 * \Delta E_{NOx}^2 + 2 * X_4 * \Delta E_{NOx} + X_5 + X_6 * r + 2 * X_7 *$$

$$r^2 * \Delta E_{NOx} + 3 * X_8 * r^3 * \Delta E_{NOx}^2 + 2 * X_9 * r * \Delta E_{NOx}^2 + 4 * X_{10} * r^3 * \Delta E_{NOx}^3 + 6 * X_{11} * r * \Delta E_{NOx}^5 + 3 * X_{12} * r * \Delta E_{NOx}^2 = 0 \quad (5)$$

Since the  $\Delta E_{NOx}$  is close to 0 when the controls are taken from the baseline, we ignore the terms of  $\Delta E_{NOx}$  in the first derivative function above, then it can be written as follows,

$$X_5 + X_6 * r = 0 \quad (6)$$

The VNr therefore can be calculated using the following equation:

$$VNr = - \frac{X_5}{X_6} \quad (7)$$

For PM<sub>2.5</sub>, the FR can be directly calculated from the polynomial function of PM<sub>2.5</sub> by estimating the second derivative of the PM<sub>2.5</sub> response to NH<sub>3</sub> emissions without considering interaction with other pollutants (Xing et al., 2018). In this study, we selected a simplified method to calculate the FR, estimated as the corresponding NH<sub>3</sub> emission ratio when the PM<sub>2.5</sub> sensitivity to NH<sub>3</sub> and NO<sub>x</sub> emissions is equal under the baseline conditions (similar to the definition in Wang et al (2011), but here we calculated the sensitivity of PM<sub>2.5</sub> instead of nitrate in this study):

$$FR = 1 + \Delta E_{NH3} \left| \frac{\partial \Delta Conc_{PM}}{\partial \Delta E_{NH3}} = \frac{\partial \Delta Conc_{PM}}{\partial \Delta E_{NOx}} \right| \Delta E_{NH3} \in [a, b], \Delta E_{NOx} = 0, \quad (8)$$

where  $\frac{\partial \Delta Conc_{PM}}{\partial \Delta E_{NH3}}$  and  $\frac{\partial \Delta Conc_{PM}}{\partial \Delta E_{NOx}}$  are the first derivatives of the  $\Delta Conc_{PM}$  to  $\Delta E_{NH3}$  and  $\Delta E_{NOx}$ , respectively, and  $\Delta E_{NH3}$  can be obtained as follows:

$$3 * X_4 * \Delta E_{NH3}^2 + (2 * X_3 - X_{10}) * \Delta E_{NH3} + X_2 - X_{11} = 0 \quad (9)$$

The FR is the NH<sub>3</sub> emissions (represented as  $1 + \Delta E_{NH3}$ ) that correspond to the inflection point between NH<sub>3</sub>-rich and -poor conditions under baseline NO<sub>x</sub> emissions. A FR greater than 1 indicates that the baseline condition is NH<sub>3</sub> poor, and a FR less than 1 indicates that the baseline condition is NH<sub>3</sub> rich. The extra benefit in PM<sub>2.5</sub> reduction (denoted as  $\Delta C_{NH3}$ ) from simultaneous NH<sub>3</sub> controls in the same percentage as the required NO<sub>x</sub> controls can be quantified as follows:



$$\Delta C_{NH_3} = \left( \frac{\partial \Delta Conc_{PM_{2.5}}}{\partial \Delta E_{NOx}} \Big|_{\Delta E_{NH_3} = \Delta E_{NOx}} \right) - \left( \frac{\partial \Delta Conc_{PM_{2.5}}}{\partial \Delta E_{NOx}} \Big|_{\Delta E_{NH_3} = 0} \right) \quad (10)$$

where

$\frac{\partial \Delta Conc_{PM_{2.5}}}{\partial \Delta E_{NOx}} \Big|_{\Delta E_{NH_3} = \Delta E_{NOx}}$  is the first derivative of the  $\Delta Conc_{PM_{2.5}}$  response to  $\Delta E_{NOx}$  when  $\Delta E_{NH_3} =$

$\Delta E_{NOx}$ , and

$\frac{\partial \Delta Conc_{PM_{2.5}}}{\partial \Delta E_{NOx}} \Big|_{\Delta E_{NH_3} = 0}$  is the first derivative of the  $\Delta Conc_{PM_{2.5}}$  response to  $\Delta E_{NOx}$  when  $\Delta E_{NH_3} = 0$ .

$\Delta C_{NH_3}$  can be calculated as follows:

$$\Delta C_{NH_3} = X_2 \quad (11)$$

### 2.3. Observable indicators of O<sub>3</sub> and PM<sub>2.5</sub> chemistry

Zhang et al. (2009) summarized the various observable indicators with their corresponding transition values to identify O<sub>3</sub> and PM<sub>2.5</sub> chemistry: O<sub>3</sub> indicators were H<sub>2</sub>O<sub>2</sub>/HNO<sub>3</sub>, H<sub>2</sub>O<sub>2</sub>/(O<sub>3</sub>+NO<sub>2</sub>), NO<sub>y</sub>, O<sub>3</sub>/NO<sub>x</sub>, O<sub>3</sub>/NO<sub>y</sub>, O<sub>3</sub>/NO<sub>z</sub>, HCHO/NO<sub>y</sub>, and HCHO/NO<sub>2</sub>, and the PM<sub>2.5</sub> indicators were the DSN, GR, and AdjGR (defined in Text S1); these indicators have been used extensively in previous research (Liu et al., 2010; Wang et al., 2011; Ye et al., 2016). In the current study, we evaluated all the aforementioned indicators except DSN (DSN is included in the definition of the AdjGR, thus it was not considered as a separate indicator in this study). The original transition values, summarized by Zhang et al (2009), are listed in Table 2. In the present study, we examined these transition values and compared their performance in predicting O<sub>3</sub> and PM<sub>2.5</sub> chemistry. Because the RSM-based indicators, PR and FR, are calculated using the multiple CTM simulations that use state-of-the-science representations of O<sub>3</sub> and PM<sub>2.5</sub> chemistry, these indicators were assumed to represent the true condition for comparison with the condition predicted using observable indicators. The performance of each observable indicator is described by its success rate, which is the ratio of the number of correct predictions to the total number of predictions. A correct prediction is indicated by the observable indicator providing consistent results for O<sub>3</sub> or PM<sub>2.5</sub> chemistry

as suggested by PR or FR. The comparison is only conducted for spatial grid cells with valid PR or FR values within the range of 0 (fully controlled emissions) to 2 (double emissions).

As RSM-based indicators, the PR and FR have meaningful values that can be used to illustrate the extent of the chemistry regime. The linkage of observable indicators with the PR and FR was investigated by performing a linear-log regression of the value of the original observable indicator and the values of the PR or FR as follows:

$$\log(Y) = A \cdot X + B \quad (12)$$

where  $Y$  is an observable indicator for  $O_3$  or  $PM_{2.5}$ ,  $X$  is the RSM-based indicator (i.e., PR for  $O_3$  or FR for  $PM_{2.5}$ ), and the coefficients  $A$  and  $B$  are estimated based on statistical regression. Therefore, the observable response indicators ( $X'$ ) can be calculated as follows:

$$X' = \frac{\log(Y) - B}{A} \quad (13)$$

The observable response indicators have the same policy implication as that of PR or FR, but they can be directly calculated from the baseline concentrations of certain chemical species rather than being derived from multiple CTM simulations. Therefore, these indicators are considerably more efficient than are traditional RSM-based indicators.

## 3. Results

### 3.1. Evaluating observable indicator performance in predicting chemistry regimes

#### 3.1.1. $O_3$

Observable indicators and the PR are compared in Fig. 4, and the performance of observable indicators in predicting  $O_3$  chemistry is summarized in Table 2. In general, strong correlation was noted between the observable indicators and PR. The indicator with the highest annual success rate was  $H_2O_2/HNO_3$  approximately 73.4 %, with a value of 0.2 for the transition from  $NO_x$ -saturated to  $NO_x$ -

291 limited conditions. However, the original transition value of 0.2 for  $\text{H}_2\text{O}_2/\text{HNO}_3$  tended to be too low,  
292 particularly in April, July, and October (see Fig. 4a). This study found that the annual success rate of  
293  $\text{H}_2\text{O}_2/\text{HNO}_3$  could be increased to 80.5 % if 0.3 was used as the transition value. This finding was  
294 consistent with corresponding findings in previous studies, which have suggested the transition values of  
295  $\text{H}_2\text{O}_2/\text{HNO}_3$  within the range of 0.2-3.6 at different locations and in different seasons (Sillman, 1995;  
296 Sillman et al, 1997; Lu and Chang, 1998; Tonnesen and Dennis, 2000; Hammer et al, 2002; Liang et al,  
297 2006; Zhang et al., 2009).  $\text{H}_2\text{O}_2/(\text{O}_3+\text{NO}_2)$ , with a transition value of 0.02, also exhibited a high annual  
298 success rate of 66.4 %; this rate could be increased to 71.1 % by applying a transition value of 0.005  
299 because the original transition value was too high, particularly in January, April, and October (see Fig. 4b).  
300  $\text{HCHO}/\text{NO}_y$  and  $\text{HCHO}/\text{NO}_2$  exhibited relatively low performance, particularly in April and July, because  
301 the original transition values appeared to be too high (Fig. 4h and i). However, the performance of  
302  $\text{HCHO}/\text{NO}_y$  and  $\text{HCHO}/\text{NO}_2$  could be greatly improved by using lower transition values, with increased  
303 annual success rates as high as 76 %. The change of the transition values implies that such indicators  
304 cannot fully consider all factors that determine the  $\text{O}_3$  chemistry by using concentrations of just two  
305 species. The transition values of the indicators  $\text{NO}_y$ ,  $\text{O}_3/\text{NO}_x$ ,  $\text{O}_3/\text{NO}_y$ , and  $\text{O}_3/\text{NO}_z$  were suitable for  
306 estimating annual levels if only one unique transition value was applied for all months (apparently, these  
307 transition values for  $\text{O}_3/\text{NO}_x$ ,  $\text{O}_3/\text{NO}_y$  and  $\text{O}_3/\text{NO}_z$  in January, and  $\text{NO}_x$  in April and July may have been  
308 too low). However, their success rates (all < 70 %) were not as high as those of other indicators. The  
309 inferior performance of the three  $\text{O}_3$ -involved indicators ( $\text{O}_3/\text{NO}_x$ ,  $\text{O}_3/\text{NO}_y$  and  $\text{O}_3/\text{NO}_z$ ) may have been  
310 associated with the considerable effects of background  $\text{O}_3$ , which cannot be removed easily.

311 Because  $\text{H}_2\text{O}_2/(\text{O}_3+\text{NO}_2)$  and  $\text{HCHO}/\text{NO}_2$  exhibited good performance in predicting  $\text{O}_3$  chemistry,  
312 this study proposed a new indicator combining these two indicators, namely  $\text{H}_2\text{O}_2 \times \text{HCHO}/\text{NO}_2$ , with a  
313 transition value of 0.3. The results suggested that this new indicator has the highest annual success rate,

namely 87.3 %, among all the indicators. Studies (Sillman, 1995; Tonnesen and Dennis, 2000) have suggested that HCHO is approximately proportional to the VOC reactivity (i.e., the weighted sum of the reactions of VOCs with OH) and that HCHO/NO<sub>2</sub> closely approximates the competition between OH reactions with VOC and NO<sub>2</sub> that is central to O<sub>3</sub> chemistry. H<sub>2</sub>O<sub>2</sub> derives from a key radical termination pathway under low NO<sub>x</sub> conditions (HO<sub>2</sub> + HO<sub>2</sub> → H<sub>2</sub>O<sub>2</sub> + O<sub>2</sub>). Comparison of H<sub>2</sub>O<sub>2</sub> with NO<sub>y</sub> or HNO<sub>3</sub>, which derives from a key radical termination pathway under high NO<sub>x</sub> conditions, OH + NO<sub>2</sub> → HNO<sub>3</sub>) represents the relative abundance of VOCs to NO<sub>x</sub>. The new hybrid indicator incorporates information from the two individual indicators and could potentially be more robust.

### 3.1.2 PM<sub>2.5</sub>

We selected the GR and AdjGR as observable indicators for PM<sub>2.5</sub> chemistry to identify NH<sub>3</sub>-poor or NH<sub>3</sub>-rich conditions. Comparison of GR and AdjGR with the FR is detailed in Fig. 5. AdjGR performance was much higher than that of the GR, with a larger annual success rate of 74.1 % compared with the GR's 55.6 % (see Table 3). The transition value of the GR appeared to be too low in all months (Fig. 5a). This result was consistent with those of previous studies; the AdjGR tends to be a more robust indicator because in contrast to the GR, it does not require an assumption of full sulfate neutralization (Zhang et al., 2009). The improvement of AdjGR compared to GR is the greatest in January and the smallest in July (Table 3). This is consistent with Pinder et al. (2008) who showed that accounting for DSN is important under cold temperatures but GR and AdjGR converge for higher temperatures.

This study designed a new indicator, total ammonia ratio (TAR), where the sulfate concentration is involved in the calculation, as follows:

$$TAR = \frac{[TA]^2}{[TN] \times [TS]} = \frac{[NH_3] \times [NH_4^+]}{([HNO_3] + [NO_3^-]) \times [SO_4^{2-}]}, \quad (14)$$

where [TN] and [TS] are the total molar concentrations of nitrate ([HNO<sub>3</sub>] + [NO<sub>3</sub><sup>-</sup>]) and sulfate

336 ( $[SO_4^{2-}]$ ), respectively, and TAR is the relative abundance of total ammonia to nitrate and sulfate, regarded  
337 as the product of  $[TA]/[TN]$  and  $[TA]/[TS]$ . To simplify the calculation,  $[TA]^2$  is assumed to be the  
338 product of the molar concentration of ammonia gas  $[NH_3]$  and ammonium  $[NH_4^+]$ .

339 The performance of TAR in predicting  $PM_{2.5}$  chemistry was slightly higher than that of AdjGR, as  
340 demonstrated by the higher success rate of TAR than that of AdjGR in all months. The annual success rate  
341 of TAR was 79.6 %, with a transition value of 10 (Table 3).

## 342 3.2 Developing the observable responsive indicators

### 343 3.2.1 $O_3$

344 Fig. 6 presents the log-linear regressions of the  $O_3$  observable indicators on the PR indicator derived  
345 from the RSM. In general, all observable indicators exhibited strong correlations with the PR (all except  
346  $NO_y$  presented positive correlations with the PR), with varying  $R^2$  values (0.08 – 0.75). The indicators  
347 including  $NO_y$ ,  $O_3/NO_x$ ,  $O_3/NO_y$ , and  $O_3/NO_z$ , which had relatively low success rates, exhibited weaker  
348 correlation with the PR ( $R^2 < 0.31$ ; Fig. 6c-f). The newly developed  $H_2O_2 \times HCHO/NO_2$  indicator exhibited  
349 the strongest correlation with the PR ( $R^2 = 0.75$ ), implying that the log-linear combination of the  $H_2O_2$ ,  
350  $HCHO$ , and  $NO_2$  baseline concentrations could approximate the responsive PR indicator to quantify  $O_3$   
351 chemistry. Other indicators can also be used to approximately estimate the PR based on the regression  
352 coefficients shown in Fig. 6; however, their correlations with the PR were not as strong as those with  
353  $H_2O_2 \times HCHO/NO_2$ .

354 To evaluate the ability of the observable PR (oPR; estimated based on  $H_2O_2 \times HCHO/NO_2$ ) to  
355 represent the spatial and temporal variation of  $O_3$  chemistry, the spatial distribution of the PR and oPR in  
356 the four study months was compared across the simulated domain (Fig. 7). The oPR successfully captured  
357 the strong  $NO_x$ -saturated regime in January ( $PR < 1$ ) and the  $NO_x$ -limited ( $PR > 1$ ) regime in July.

358 In addition, the PR and oPR suggested a consistently strong NO<sub>x</sub>-saturated regime in northern and  
359 eastern China and key regions such as the YRD and PRD. The domain-averaged oPRs were 0.97, 1.52,  
360 1.73, and 1.37 in January, April, July, and October, respectively; these values are similar to the PRs (0.77,  
361 1.24, 1.38, and 1.17, respectively). Thus, the oPR may approximate the PR to quantify the O<sub>3</sub> chemistry,  
362 even on a large spatial and temporal scale.

### 363 3.2.2. PM<sub>2.5</sub>

364 The correlations between PM<sub>2.5</sub> observable indicators and the responsive FR indicator derived from  
365 the RSM were investigated (Fig. 8). The AdjGR has the lowest R<sup>2</sup> (0.40) because of its high variations for  
366 the NH<sub>3</sub>-poor condition (Fig. 5b). A stronger positive correlation was noted between the GR and FR (R<sup>2</sup>  
367 = 0.57); however, the success rate of the GR was the lowest among all the indicators (the success rate of  
368 the GR increased when the transition value was set as the median value of the GR, namely 5, at an FR of  
369 1). The TAR exhibited the strongest positive correlation with the FR (R<sup>2</sup> = 0.60), implying that the FR can  
370 be approximately estimated by the log-linear combination of baseline concentrations of ammonia gas,  
371 nitric acid gas, particulate ammonium, sulfate, and nitrate.

372 The capability of the observable FR (oFR; estimated based on the TAR indicator) in representing  
373 the spatial and temporal variation of PM<sub>2.5</sub> chemistry is illustrated in Fig. 9. Both the FR and oFR  
374 suggested strong NH<sub>3</sub>-poor condition (FR > 1) in January and NH<sub>3</sub>-rich condition (FR < 1) in April and  
375 July. The oFR suggested strong NH<sub>3</sub>-rich condition in northern and eastern China and the Sichuan Basin;  
376 these findings were consistent with those for the FR. The domain-averaged oFRs were 1.56, 1.05, 0.86,  
377 and 1.24 in January, April, July, and October, respectively, with the strongest NH<sub>3</sub>-poor condition in  
378 January and NH<sub>3</sub>-rich condition in July. These findings were comparable with the FRs of 1.47, 1.16, 0.95,  
379 and 1.19 for the four study months, respectively, suggesting that the oFR can approximate the FR to  
380 quantify the PM<sub>2.5</sub> chemistry and its spatial and temporal variations.

### 3.3. Policy implications

#### 3.3.1. O<sub>3</sub>

The responsive PR indicator may help policy-makers to understand the status and extent of O<sub>3</sub> chemistry in the current scenarios. A lower PR ( $< 1$ ) suggested a NO<sub>x</sub>-saturated regime. Moreover, the VNr could be used to inform policy-makers about the level of simultaneous control of VOCs required to prevent an increase in O<sub>3</sub> levels from NO<sub>x</sub> controls. In general, the VNr is negatively correlated with the PR because a lower PR implies a stronger NO<sub>x</sub>-saturated regime, which in turn requires more simultaneous VOC control with NO<sub>x</sub>. By contrast, a higher PR implies a weaker NO<sub>x</sub>-saturated or even NO<sub>x</sub>-limited regime, which requires less or no simultaneous control of VOCs with NO<sub>x</sub>. The negative correlation between VNr and the PR was quantified by the simple linear regression of VNr on PR (Fig. S7). A high R<sup>2</sup> (approximately 0.82) suggested that the VNr originally derived from the RSM can also be approximately estimated from the PR or oPR.

Figure 10 presents a comparison of the VNr derived from the RSM, with the VNr calculated based on the oPR, estimated by the H<sub>2</sub>O<sub>2</sub>×HCHO/NO<sub>2</sub> indicator and denoted as oVNr. Consistent spatial and temporal variations were found for VNr and oVNr. Additional simultaneous VOC control is required in January and in northern and eastern China, and is highly correlated with the low PR (Fig. 7). The domain-averaged oVNr values were estimated to be 0.95, 0.43, 0.38, and 0.47 in January, April, July, and October, respectively, with the highest and lowest oVNr values noted in January and July, respectively. That is comparable with VNr in the four study months (i.e., 0.82, 0.46, 0.34, and 0.57, respectively).

The annual-averaged VNr and PR were also calculated for each province in China (Fig. 11). VNr was negatively correlated with the PR at the provincial level. The northern provinces, namely Heilongjiang, Xinjiang, and Liaoning required the highest VNr (1-1.2) because their PRs were very low (0.3-0.4). In the NCP, including the province of Tianjin, Hebei, Henan, Shandong, Shanxi, Inner Mongolia, and Beijing,

high VNr (0.7-0.9) was required to overcome the stronger NO<sub>x</sub>-saturated regime (PR = 0.4-0.6). The coastal provinces, namely Fujian, and Guangdong, and middle-eastern provinces, namely Jiangxi and Hunan, also demonstrated relatively high PRs (>0.7) and low VNr (<0.3).

### 3.3.2. PM<sub>2.5</sub>

Using the responsive FR indicator or its observable oFR indicator can rapidly identify NH<sub>3</sub>-rich or NH<sub>3</sub>-poor conditions, and this information can aid policy-makers in estimating the additional PM<sub>2.5</sub> benefit associated with simultaneous control of NH<sub>3</sub> and NO<sub>x</sub> emissions ( $\Delta C_{NH_3}$ ). As discussed in Section 2.2,  $\Delta C_{NH_3}$  can be calculated from the RSM using the first derivative of the PM<sub>2.5</sub> responsive function to NH<sub>3</sub>. Therefore,  $\Delta C_{NH_3}$  must be strongly associated with the secondary inorganic aerosol (SNA) concentration, as suggested in Fig. S8, which demonstrates a strong correlation between SNA concentration and  $\Delta C_{NH_3}$ . The linear regression with high R<sup>2</sup> (>0.71) implies that the  $\Delta C_{NH_3}$  can be approximately calculated based on the SNA concentration.

The  $\Delta C_{NH_3}$  estimated based on the SNA concentration (o $\Delta C_{NH_3}$ ; based on the regression function in Fig. S8) was compared with that derived from the RSM (Fig. 12). The o $\Delta C_{NH_3}$  typically captured the spatial and temporal variation of  $\Delta C_{NH_3}$ , suggesting large benefits in January and October, particularly in eastern China and the Sichuan Basin. The domain-averaged  $\Delta C_{NH_3}$  values were approximately 0.31, 0.22, 0.16, and 0.38  $\mu\text{g m}^{-3}$  PM<sub>2.5</sub> per 10 % NH<sub>3</sub> reduction in January, April, July, and October respectively. In April and July, o $\Delta C_{NH_3}$  presented consistent results approximately 0.21 and 0.16  $\mu\text{g m}^{-3}$  PM<sub>2.5</sub>, respectively, per 10 % NH<sub>3</sub> reduction, but slightly underestimated the benefits in January and October (0.24 and 0.22  $\mu\text{g m}^{-3}$  PM<sub>2.5</sub>, respectively, per 10 % NH<sub>3</sub> reduction).

At the annual level,  $\Delta C_{NH_3}$  was compared with the population-weighted PM<sub>2.5</sub> concentration in each province (Fig. 13).  $\Delta C_{NH_3}$  ranged from 2 to 12  $\mu\text{g m}^{-3}$  PM<sub>2.5</sub> per 10 % NH<sub>3</sub> reduction. In addition, the provinces with higher PM<sub>2.5</sub> exposure exhibited additional benefits from NH<sub>3</sub> reductions (i.e., high



427  $\Delta C_{\text{NH}_3}$ ), particularly in Hunan, Shandong, Tianjin, Jiangxi, Anhui, Henan, and Hubei where  $\Delta C_{\text{NH}_3}$   
428 was  $> 8 \mu\text{g m}^{-3}$   $\text{PM}_{2.5}$  per 10 %  $\text{NH}_3$  reduction. These benefits from simultaneous  $\text{NH}_3$  control were  
429 substantial enough to be considered in these regions for achieving the national ambient  $\text{PM}_{2.5}$  target ( $35$   
430  $\mu\text{g m}^{-3}$ ).

### 431 3.3.3. Cobenefits of $\text{NO}_x$ and VOC control in reducing $\text{O}_3$ and $\text{PM}_{2.5}$

432  $\text{NO}_x$  and VOCs are major precursors for  $\text{O}_3$  and  $\text{PM}_{2.5}$ , and effectively controlling their emissions  
433 can lead to cobenefits in reducing  $\text{O}_3$  and  $\text{PM}_{2.5}$ . The PR results suggest strong  $\text{NO}_x$ -saturated regimes in  
434 northern and eastern China including key regions such as the Sichuan Basin, YRD, and PRD, where  
435 simultaneous VOC control with a certain VOC-to- $\text{NO}_x$  ratio is required to prevent increases in  $\text{O}_3$  levels  
436 from the  $\text{NO}_x$  controls.  $\text{PM}_{2.5}$  sensitivity to  $\text{NO}_x$  can be negative under a strong  $\text{NO}_x$ -saturated regime; this  
437 effect is not as significant as it is for  $\text{O}_3$  (Fig. 3). We quantified the nonlinearity of  $\text{PM}_{2.5}$  sensitivity to  $\text{NO}_x$   
438 by using the same PR concept but for  $\text{PM}_{2.5}$  response (Text S2); Fig. S9 presents the spatial distribution  
439 of the PR to identify  $\text{PM}_{2.5}$  sensitivity to  $\text{NO}_x$  emission in the four study months. The PR values for  $\text{PM}_{2.5}$   
440 were  $> 1$  in April, July, and October in all grid cells across China, suggesting that  $\text{NO}_x$  control is always  
441 beneficial for  $\text{PM}_{2.5}$  reduction during these months. Even in January, the PR for  $\text{PM}_{2.5}$  (0.4-0.8 in eastern  
442 and northern China) remains larger than that for  $\text{O}_3$  (0.2-0.6 in eastern and northern China), implying that  
443 the suggested VNr for  $\text{O}_3$  was high enough to overcome the potential limitations on  $\text{PM}_{2.5}$  reduction from  
444  $\text{NO}_x$  control.

445 To explore the cobenefits of reducing  $\text{O}_3$  and  $\text{PM}_{2.5}$  after simultaneous control of  $\text{NO}_x$  and VOCs,  
446 we investigated the effectiveness of six control pathways with various VOC-to- $\text{NO}_x$  ratios including 0,  
447 0.2, 0.4, 0.6, 0.8 and 1.0 (Fig. 14). In general,  $\text{O}_3$  and  $\text{PM}_{2.5}$  concentrations can be reduced in all months  
448 through simultaneous control of  $\text{NO}_x$  and VOC emissions, although different VNr and control levels are  
449 required in different months. In January (under strongly  $\text{NO}_x$ -saturated conditions), reductions in  $\text{PM}_{2.5}$

and O<sub>3</sub> require VOC emission controls in addition to NO<sub>x</sub> controls to prevent potential disbenefits associated with the nonlinear chemistry. The smaller VNr required for PM<sub>2.5</sub> (~0.4) than for O<sub>3</sub> (~1.0) in this case might be associated with the smaller PR for PM<sub>2.5</sub> as well as the additional benefit of VOC controls in reducing secondary organic aerosols. Apparently, a larger VNr control ratio and greater emission control is required in January compared with other months. In Fig. 14(a), only one pathway can achieve simultaneous reduction in O<sub>3</sub> and PM<sub>2.5</sub> concentrations (i.e., the pathway with VNr equal to 1 and at the far end of the pathway, with reduction rates > 80%). In April and October, simultaneous VOC controls were still required for O<sub>3</sub> (VNr = 0.2-0.6) but not for PM<sub>2.5</sub>. In July when NO<sub>x</sub>-limited regime was dominant, the NO<sub>x</sub> control was critical because the VOC controls had little effect on either O<sub>3</sub> or PM<sub>2.5</sub>. At the annual level, the simultaneous VOC controls (40 % of the NO<sub>x</sub> controls) led to cobenefits in reducing both O<sub>3</sub> and PM<sub>2.5</sub> at the national level. However, VNr varied significantly in different seasons, suggesting that considering the seasonality of O<sub>3</sub> and PM<sub>2.5</sub> chemistry is necessary for design of a season-specific control strategy.

## 4. Summary and conclusion

Compared with conducting multiple CTM simulations, the indicator method proved more efficient in identifying the chemical regime in the current scenarios. However, the traditional indicators are not as useful as the RSM-based PR and FR indicators for policy-makers to infer feasible emission reduction paths. Therefore, this study quantified the relationship between RSM-based and traditional-observable indicators and developed new observable response indicators, the oPR and oFR, which can be used to quantify the nonlinearity of O<sub>3</sub> and PM<sub>2.5</sub> response to precursor emissions. Similar to the traditional indicators, the oPR and oFR can be easily calculated using a combination of ambient concentrations of certain chemical species obtained from surface-monitored observations, modeling simulations, or even satellite retrievals. In addition, the observable responsive indicators can not only rapidly identify the

473 chemical regime but also provide policy-makers with useful information, such as simultaneous VOC  
474 controls to prevent increases in  $O_3$  levels from  $NO_x$  controls under the  $NO_x$ -saturated regime (i.e., VNr),  
475 as well as the additional benefit of simultaneously reducing  $NH_3$  alongside  $NO_x$  control in  $PM_{2.5}$  reductions  
476 (i.e.,  $\Delta C_{NH_3}$ ). Since the indicators are developed from simulations with spatially uniform emission  
477 controls across the country, they are especially useful for providing quick estimates of the potential  
478 benefits or risks from uniform controls. These estimates can also provide a basis to design more localized  
479 control strategies for particular regions.

480 This study proposed a new  $O_3$ -chemistry indicator, namely  $H_2O_2 \times HCHO / NO_2$ , and  $PM_{2.5}$ -chemistry  
481 indicator, namely the TAR, both of which exhibited the highest success rates among all the indicators.  
482 This study also suggested that the log-linear combinations of baseline  $H_2O_2$ ,  $HCHO$ , and  $NO_2$   
483 concentrations could provide an approximate PR to quantify  $O_3$  chemistry spatially and temporally.  
484 Similarly, the log-linear combination of baseline concentrations of ammonia gas, nitric acid gas,  
485 particulate ammonium, sulfate and nitrate can be used to approximately estimate the FR for  $PM_{2.5}$   
486 chemistry. The VNr was highly correlated with the PR, suggesting that a stronger  $NO_x$ -saturated regime  
487 requires greater VOC control accompanied by  $NO_x$  control. The positive correlation between  $\Delta C_{NH_3}$   
488 and the population-weighted  $PM_{2.5}$  concentration suggested that a province with high  $PM_{2.5}$  exposure can  
489 gain greater benefits from  $NH_3$  reduction. Finally, simultaneous control of  $NO_x$  and VOC could reduce  
490 both  $O_3$  and  $PM_{2.5}$  throughout the year, and an effective control pathway (VNr = 0.4) could lead to the  
491 cobenefits of reducing both  $O_3$  and  $PM_{2.5}$ . However, VNr varied significantly among the seasons and  
492 provinces, suggesting the necessity of considering the seasonality of chemistry and of designing a more  
493 localized control strategy for each province. We note that the discrepancy between the observable indicator  
494 and the responsive indicator might also be influenced by uncertainties in the chemical mechanism of  
495 CMAQ as well as prediction errors of the pf-RSM. The new indicators were designed based on the existing

chemical mechanism, and the transition values might be refined in the future as our understanding of atmospheric chemical processes improves.

In conclusion, the two unique aspects of this study are as follows. First, quantification of the correlation of observable indicators with responsive indicators (Fig. 5 and 7) implied that the traditional observable indicators, based on monitored or satellite-retrieved concentrations, can be used to quantify the nonlinearity of  $\text{PM}_{2.5}$  and  $\text{O}_3$  to precursor emission and provide useful policy implications. Second, this study reported a promising method for efficiently establishing  $\text{PM}_{2.5}$ - and  $\text{O}_3$ - responsive functions to precursors for traditional responsive or reduced-form modeling studies. This study suggested that the PR or FR (a combination of coefficients in the polynomial functions in the pf-RSM) can be approximately estimated using the ambient concentration of certain chemical species. Similarly, all coefficients in polynomial functions can be calculated based on a set of ambient concentrations of certain chemical species. The simple log-linear regression method used in this study demonstrated the possibility that even in the presence of uncertainties in prediction, more advanced data analytics technologies such as deep learning may improve performance in future.

## Data availability

The pf-RSM outputs and code package are available upon request from the corresponding author.

## Author contribution

These authors contributed equally to this work: Jia Xing & Dian Ding. JX designed the methodology and wrote the paper. DD conducted the modeling experiment and analyzed the data. SW provided ideas and financial support and edited the paper. ZD and YZ helped with the modeling experiment. JK, CJ and JH provided ideas and edited the paper.

## Acknowledgements

This work was supported in part by National Key R & D program of China (2017YFC0210006), National Natural Science Foundation of China (21625701&51861135102), National Research Program for Key Issues in Air Pollution Control (DQGG0301& DQGG0204), and Shanghai Environmental Protection Bureau (2016-12). This work was completed on the “Explorer 100” cluster system of Tsinghua National Laboratory for Information Science and Technology.

## Disclaimer

Although this work was reviewed by EPA and approved for publication, the views in the article are those of the authors alone and do not necessarily reflect the policy of the Agency. Mention of commercial products does not constitute endorsement by the Agency.

## Reference

- Ansari, A. S., and S. N. Pandis: Response of inorganic PM to precursor concentrations, *Environ. Sci. Technol.*, 32, 2706–2714, 1998.
- Cohan, D.S., Hakami, A., Hu, Y., Russell, A.G.: Nonlinear response of ozone to emissions: source apportionment and sensitivity analysis. *Environ. Sci. Technol.*, 39, 6739-6748, 2005.
- Cohen, A.J., Brauer, M., Burnett, R., Anderson, H.R., Frostad, J., Estep, K., Balakrishnan, K., Brunekreef, B., Dandona, L., Dandona, R., Feigin, V.: Estimates and 25-year trends of the global burden of disease attributable to ambient air pollution: an analysis of data from the Global Burden of Diseases Study 2015. *The Lancet*, 389(10082), 1907-1918, 2017.
- Dennis, R.L., Bhawe, P.V. and Pinder, R.W. Observable indicators of the sensitivity of PM<sub>2.5</sub> nitrate to emission reductions—Part II: Sensitivity to errors in total ammonia and total nitrate of the CMAQ-predicted non-linear effect of SO<sub>2</sub> emission reductions. *Atmospheric Environment*, 42(6), pp.1287-1300, 2008.
- Ding, D., Xing, J., Wang, S., Liu, K. and Hao, J.: Estimated Contributions of Emissions Controls, Meteorological Factors, Population Growth, and Changes in Baseline Mortality to Reductions in Ambient PM<sub>2.5</sub> and PM<sub>2.5</sub>-Related Mortality in China, 2013–2017. *Environmental health perspectives*, 127(6), 067009, 2019a.

548 Ding, D., Xing, J., Wang, S., Chang, X. and Hao, J.: Impacts of emissions and meteorological changes on  
 549 China's ozone pollution in the warm seasons of 2013 and 2017, *Front. Environ. Sci. Eng.* 2019,  
 550 13(5): 76, 2019b.

551 Forouzanfar, M.H., Alexander, L., Anderson, H.R., Bachman, V.F., Biryukov, S., Brauer, M., Burnett, R.,  
 552 Casey, D., Coates, M.M., Cohen, A., Delwiche, K.: Global, regional, and national comparative risk  
 553 assessment of 79 behavioural, environmental and occupational, and metabolic risks or clusters of  
 554 risks in 188 countries, 1990–2013: a systematic analysis for the Global Burden of Disease Study  
 555 2013. *The Lancet*, 386 (10010), 2287–2323, 2015.

556 Freas, W. P., Martinez, E. L., Meyer, E. L., Possiel, N. C., and Sennett, D. H.: Procedures for quantifying  
 557 relationships between photochemical oxidants and precursors: supporting documentation, 1978.

558 Friedlander, S.K. Smoke, dust and haze: Fundamentals of aerosol behavior. New York, Wiley-Interscience,  
 559 1977. 333pp.

560 Fuhrer, J., Val Martin, M. , Mills, G. , Heald, C.L., Harmens, H., Hayes, F., Sharps, K., Bender, J., Ashmore,  
 561 M.R.: Current and future ozone risks to global terrestrial biodiversity and ecosystem processes.  
 562 *Ecology and evolution*, 6(24), 8785-8799, 2016.

563 Gipson, G. L., Freas, W. P., Kelly, R. F., and Meyer, E. L.: Guideline for use of city-specific EKMA in  
 564 preparing ozone SIPs. EPA-450/4-80-027, US Environmental Protection Agency, Research  
 565 Triangle Park, North Carolina, USA, 1981.

566 Hakami, A., Odman, M.T., Russell, A.G.: Nonlinearity in atmospheric response: A direct sensitivity  
 567 analysis approach. *Journal of Geophysical Research: Atmospheres*, 109(D15), 2004.

568 Hammer, M.U., Vogel, B. and Vogel, H.: Findings on H<sub>2</sub>O<sub>2</sub>/HNO<sub>3</sub> as an indicator of ozone sensitivity in  
 569 Baden-Württemberg, Berlin-Brandenburg, and the Po valley based on numerical simulations.  
 570 *Journal of Geophysical Research: Atmospheres*, 107(D22), 2002.

571 Jiménez, P. and Baldasano, J.M.: Ozone response to precursor controls in very complex terrains: Use of  
 572 photochemical indicators to assess O<sub>3</sub>-NO<sub>x</sub>-VOC sensitivity in the northeastern Iberian Peninsula.  
 573 *Journal of Geophysical Research: Atmospheres*, 109(D20), 2004.

574 Jin, X., Fiore, A.M., Murray, L.T., Valin, L.C., Lamsal, L.N., Duncan, B., Folkert Boersma, K., De Smedt,  
 575 I., Abad, G.G., Chance, K. and Tonnesen, G.S.: Evaluating a Space-Based Indicator of Surface  
 576 Ozone-NO<sub>x</sub>-VOC Sensitivity Over Midlatitude Source Regions and Application to Decadal  
 577 Trends. *Journal of Geophysical Research: Atmospheres*, 122(19), 2017.

578 Li, K., Jacob, D.J., Liao, H., Shen, L., Zhang, Q. and Bates, K.H.: Anthropogenic drivers of 2013–2017  
 579 trends in summer surface ozone in China. *Proceedings of the National Academy of*  
 580 *Sciences*, 116(2), pp.422-427, 2019.

581 Liang, J., Jackson, B. and Kaduvela, A.: Evaluation of the ability of indicator species ratios to determine  
 582 the sensitivity of ozone to reductions in emissions of volatile organic compounds and oxides of  
 583 nitrogen in northern California. *Atmospheric Environment*, 40(27), pp.5156-5166, 2006.

584 Liu, X.H., Zhang, Y., Xing, J., Zhang, Q., Wang, K., Streets, D.G., Jang, C., Wang, W.X., Hao, J.M.:  
 585 Understanding of regional air pollution over China using CMAQ, part II. Process analysis and  
 586 sensitivity of ozone and particulate matter to precursor emissions. *Atmospheric Environment*,  
 587 44(30), 3719-3727, 2010.

588 Lu, C.H. and Chang, J.S.: On the indicator-based approach to assess ozone sensitivities and emissions  
 589 features. *Journal of Geophysical Research: Atmospheres*, 103(D3), pp.3453-3462, 1998.

590 Lu, X., Hong, J., Zhang, L., Cooper, O. R., Schultz, M. G., Xu, X., Wang, T., Gao, M., Zhao, Y., and  
 591 Zhang, Y.: Severe Surface Ozone Pollution in China: A Global Perspective, *Environmental Science*  
 592 *& Technology Letters*, 5, 487-494, 10.1021/acs.estlett.8b00366, 2018.

593 Megaritis, A.G., Fountoukis, C., Charalampidis, P.E., Pilinis, C. and Pandis, S.N.: Response of fine  
 594 particulate matter concentrations to changes of emissions and temperature in Europe. *Atmospheric*  
 595 *Chemistry and Physics*, 13(6), 3423-3443, 2013.

596 Milford, J. B., Gao, D. F., Sillman, S., Blossy, P., and Russell, A. G.: Total reactive nitrogen (NO<sub>y</sub>) as  
 597 an indicator of the sensitivity of ozone to reductions in hydrocarbon and NO<sub>x</sub> emissions, *Journal*  
 598 *of Geophysical Research-Atmospheres*, 99, 3533-3542, 10.1029/93jd03224, 1994.

599 Myhre, G., Shindell, D., Bréon, F.M., Collins, W., Fuglestad, J., Huang, J., Koch, D., Lamarque, J.F.,  
 600 Lee, D., Mendoza, B., Nakajima, T. Anthropogenic and Natural Radiative Forcing. In: *Climate*  
 601 *Change 2013: The Physical Science Basis. Contribution of Working Group I to the Fifth*  
 602 *Assessment Report of the Intergovernmental Panel on Climate Change*, T.F. Stocker et al, Eds.  
 603 Cambridge Univ. Press, 2013, 659-740.

604 Oak Ridge National Laboratory. Landsat global population dataset 2012. Oak Ridge, Tennessee: Oak  
 605 Ridge National Laboratory, 2013

606 Peng, Y.P., Chen, K.S., Lai, C.H., Lu, P.J. and Kao, J.H.: Concentrations of H<sub>2</sub>O<sub>2</sub> and HNO<sub>3</sub> and O<sub>3</sub>–  
 607 VOC–NO<sub>x</sub> sensitivity in ambient air in southern Taiwan. *Atmospheric Environment*, 40(35),  
 608 pp.6741-6751, 2006.

609 Pinder, R.W., Dennis, R.L. and Bhavsar, P.V.: Observable indicators of the sensitivity of PM<sub>2.5</sub> nitrate to  
 610 emission reductions—Part I: Derivation of the adjusted gas ratio and applicability at regulatory-  
 611 relevant time scales. *Atmospheric Environment*, 42(6), pp.1275-1286, 2008.

612 Pun, B.K., Seigneur, C., Bailey, E.M., Gautney, L.L., Douglas, S.G., Haney, J.L., Kumar, N.: Response of  
 613 atmospheric particulate matter to changes in precursor emissions: a comparison of three air quality  
 614 models. *Environmental science & technology*, 42(3), 831-837, 2007.

615 Seinfeld, J.H. and Pandis, S.N.: *Atmospheric chemistry and physics: from air pollution to climate change*.  
 616 John Wiley & Sons, 2012.

617 Sillman, S.: The use of NO<sub>y</sub>, H<sub>2</sub>O<sub>2</sub>, and HNO<sub>3</sub> as indicators for ozone–NO<sub>x</sub>–hydrocarbon sensitivity in  
 618 urban locations. *Journal of Geophysical Research: Atmospheres*, 100(D7), pp.14175-14188., 1995.

619 Sillman, S., He, D., Cardelino, C. and Imhoff, R.E.: The use of photochemical indicators to evaluate  
 620 ozone–NO<sub>x</sub>–hydrocarbon sensitivity: Case studies from Atlanta, New York, and Los  
 621 Angeles. *Journal of the Air & Waste Management Association*, 47(10), pp.1030-1040, 1997.

622 Sillman, S., and D. He, Some theoretical results concerning O<sub>3</sub>–NO<sub>x</sub>–VOC chemistry and NO<sub>x</sub>–VOC  
 623 indicators, *J. Geophys. Res.*, 107(D22), 4659, doi:10.1029/2001JD001123, 2002.

624 Sun, Y., Liu, C., Palm, M., Vigouroux, C., Notholt, J., Hu, Q., Jones, N., Wang, W., Su, W., Zhang, W.,  
 625 Shan, C., Tian, Y., Xu, X., De Mazière, M., Zhou, M., and Liu, J.: Ozone seasonal evolution and  
 626 photochemical production regime in the polluted troposphere in eastern China derived from high-  
 627 resolution Fourier transform spectrometry (FTS) observations, *Atmos. Chem. Phys.*, 18, 14569-  
 628 14583, <https://doi.org/10.5194/acp-18-14569-2018>, 2018.

629 Takahama, S., Wittig, A.E., Vayenas, D.V., Davidson, C.I. and Pandis, S.N.: Modeling the diurnal variation  
 630 of nitrate during the Pittsburgh Air Quality Study. *Journal of Geophysical Research: Atmospheres*,  
 631 109(D16), 2004.

632 Tonnesen, G.S. and Dennis, R.L.: Analysis of radical propagation efficiency to assess ozone sensitivity to  
 633 hydrocarbons and NO<sub>x</sub>: 2. Long-lived species as indicators of ozone concentration sensitivity.  
 634 *Journal of Geophysical Research: Atmospheres*, 105(D7), pp.9227-9241, 2000.

635 Wang, J., Xing, J., Mathur, R., Pleim, J.E., Wang, S., Hogrefe, C., Gan, C.M., Wong, D.C., Hao, J.:  
 636 Historical trends in PM<sub>2.5</sub>-related premature mortality during 1990–2010 across the northern  
 637 hemisphere. *Environmental health perspectives*, 125(3), 400pp, 2017.

- Wang, S. X., Xing, J., Jang, C., Zhu, Y., Fu, J.S., Hao, J.: Impact assessment of ammonia emissions on inorganic aerosols in east China using response surface modeling technique. *Environ. Sci. Technol.*, 45, 9293–9300, 2011.
- Wang, S., Zhao, M., Xing, J., Wu, Y., Zhou, Y., Lei, Y., He, K., Fu, L., & Hao, J.: Quantifying the air pollutants emission reduction during the 2008 Olympic Games in Beijing. *Environmental science & technology*, 44(7), 2490-2496, 2010.
- West, J.J., Ansari, A.S., Pandis, S.N. Marginal PM<sub>2.5</sub>: nonlinear aerosol mass response to sulfate reductions in the Eastern United States. *Journal of the Air & Waste Management Association*, 49(12), 1415-1424, 1999.
- Xing, J., Wang, S. X., Jang, C., Zhu, Y., and Hao, J. M.: Nonlinear response of ozone to precursor emission changes in China: a modeling study using response surface methodology, *Atmospheric Chemistry and Physics*, 11, 5027-5044, 10.5194/acp-11-5027-2011, 2011.
- Xing, J., Ding, D., Wang, S., Zhao, B., Jang, C., Wu, W., Zhang, F., Zhu, Y., and Hao, J. Quantification of the enhanced effectiveness of NO<sub>x</sub> control from simultaneous reductions of VOC and NH<sub>3</sub> for reducing air pollution in the Beijing–Tianjin–Hebei region, China, *Atmos. Chem. Phys.*, 18, 7799-7814, <https://doi.org/10.5194/acp-18-7799-2018>, 2018.
- Xing, J., Wang, S., Zhao, B., Wu, W., Ding, D., Jang, C., Zhu, Y., Chang, X., Wang, J., Zhang, F. and Hao, J.: Quantifying Nonlinear Multiregional Contributions to Ozone and Fine Particles Using an Updated Response Surface Modeling Technique. *Environmental science & technology*, 51(20), 11788-11798, 2017.
- Xing, J., Zhang, F., Zhou, Y., Wang, S., Ding, D., Jang, C., Zhu, Y. and Hao, J.: Least-cost control strategy optimization for air quality attainment of Beijing–Tianjin–Hebei region in China. *Journal of environmental management*, 245, 95-104, 2019.
- Ye, L., Wang, X., Fan, S., Chen, W., Chang, M., Zhou, S., Wu, Z. and Fan, Q.: Photochemical indicators of ozone sensitivity: application in the Pearl River Delta, China. *Frontiers of Environmental Science & Engineering*, 10(6), p.15, 2016.
- Zhang, J., Wang, T., Chameides, W. L., Cardelino, C., Kwok, J., Blake, D. R., Ding, A., and So, K. L.: Ozone production and hydrocarbon reactivity in Hong Kong, Southern China, *Atmos. Chem. Phys.*, 7, 557-573, <https://doi.org/10.5194/acp-7-557-2007>, 2007.
- Zhang, Y., Wen, X. Y., Wang, K., Vijayaraghavan, K., and Jacobson, M. Z.: Probing into regional O<sub>3</sub> and particulate matter pollution in the United States: 2. An examination of formation mechanisms through a process analysis technique and sensitivity study, *Journal of Geophysical Research-Atmospheres*, 114, 31, 10.1029/2009jd011900, 2009.
- Zhao, B., Wang, S.X., Xing, J., Fu, K., Fu, J.S., Jang, C., Zhu, Y., Dong, X.Y., Gao, Y., Wu, W.J., Wang, J.D.: Assessing the nonlinear response of fine particles to precursor emissions: development and application of an extended response surface modeling technique v1.0. *Geosci. Model Dev.*, 8, 115-128, 2015.
- Zhao, B., Zheng, H., Wang, S., Smith, K.R., Lu, X., Aunan, K., Gu, Y., Wang, Y., Ding, D., Xing, J. and Fu, X. Change in household fuels dominates the decrease in PM<sub>2.5</sub> exposure and premature mortality in China in 2005–2015. *Proceedings of the National Academy of Sciences*, 115(49), pp.12401-12406, 2018.



681

682

**Table 1.** Terms in the pf-RSM design for O<sub>3</sub> and PM<sub>2.5</sub>

Term	O <sub>3</sub>	PM <sub>2.5</sub>
1	NO <sub>x</sub> <sup>5</sup>	VOC
2	NO <sub>x</sub> <sup>4</sup>	NH <sub>3</sub>
3	NO <sub>x</sub> <sup>3</sup>	NH <sub>3</sub> <sup>2</sup>
4	NO <sub>x</sub> <sup>2</sup>	NH <sub>3</sub> <sup>3</sup>
5	NO <sub>x</sub>	SO <sub>2</sub>
6	VOC	VOC <sup>2</sup>
7	VOC <sup>2</sup>	NO <sub>x</sub> VOC
8	VOC <sup>3</sup>	NO <sub>x</sub> <sup>2</sup> VOC
9	NO <sub>x</sub> VOC	NO <sub>x</sub> <sup>4</sup> VOC
10	NO <sub>x</sub> VOC <sup>3</sup>	NO <sub>x</sub> NH <sub>3</sub>
11	NO <sub>x</sub> <sup>5</sup> VOC	NO <sub>x</sub>
12	NO <sub>x</sub> <sup>2</sup> VOC	NO <sub>x</sub> <sup>2</sup>
13	SO <sub>2</sub>	NO <sub>x</sub> <sup>3</sup>
14	NH <sub>3</sub>	NO <sub>x</sub> <sup>4</sup>

683

684

685

686 **Table 2.** Summary of observable indicators and their performances in predicting O<sub>3</sub> chemistry

Indicator	TV*	success rate at TV (%)					TV'	success rate at TV' (%)				
		Jan	Apr	Jul	Oct	ANN		Jan	Apr	Jul	Oct	ANN
H <sub>2</sub> O <sub>2</sub> /HNO <sub>3</sub>	0.2	68.8	74.9	89.0	60.8	73.4	<b>0.3</b>	77.9	83.0	90.4	70.6	80.5
H <sub>2</sub> O <sub>2</sub> /(O <sub>3</sub> +NO <sub>2</sub> )	0.02	81.1	41.9	85.4	57.4	66.4	<b>0.005</b>	69.2	73.3	88.8	53.3	71.1
NO <sub>y</sub>	5	38.9	47.8	87.8	40.9	53.8	-	-	-	-	-	-
O <sub>3</sub> /NO <sub>x</sub>	15	56.5	75.8	58.8	71.7	65.7	-	-	-	-	-	-
O <sub>3</sub> /NO <sub>y</sub>	7	60.7	65.8	23.3	68.2	54.5	-	-	-	-	-	-
O <sub>3</sub> /NO <sub>z</sub>	7	43.5	75.0	76.4	67.0	65.5	-	-	-	-	-	-
HCHO/NO <sub>y</sub>	0.28	83.9	32.5	19.4	50.9	46.7	<b>0.1</b>	66.7	77.7	86.3	75.6	76.6
HCHO/NO <sub>2</sub>	1	87.3	49.7	27.4	73.8	59.6	<b>0.5</b>	75.7	77.2	69.1	82.2	76.1
H <sub>2</sub> O <sub>2</sub> ×HCHO/NO <sub>2</sub>	-	-	-	-	-	-	<b>0.3</b>	92.3	81.6	89.5	86.0	87.3

687 \* TV- transition value as summaried in Zhang et al (2009); TV' - transition value proposed in this study

688

689

690

691 **Table 3.** Summary of observable indicators and their performances in predicting PM<sub>2.5</sub> chemistry

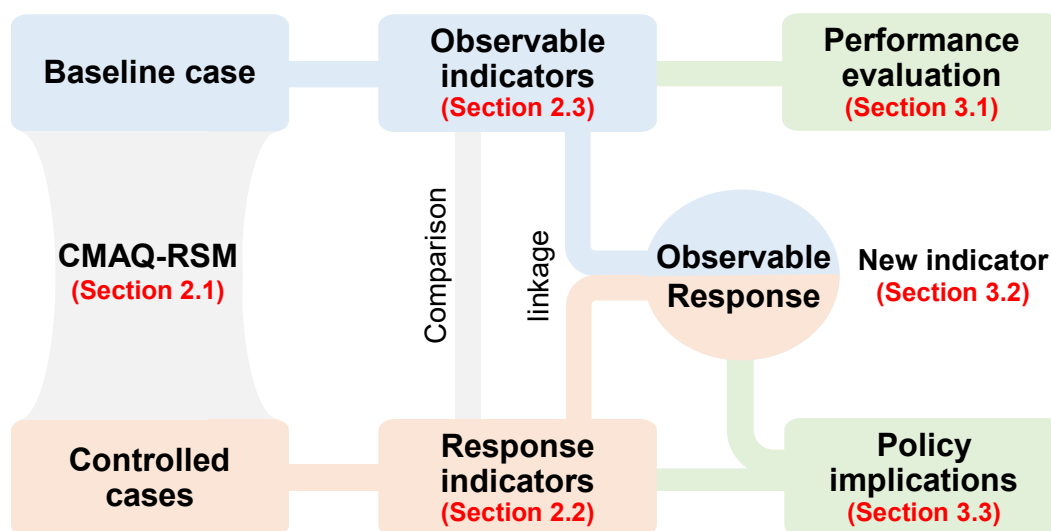
Indicator	TV	success rate (%)				
		Jan	Apr	Jul	Oct	ANN
Gas ratio (GR)	1*	51.7	59.3	69.6	41.7	55.6
Adjusted Gas ratio (AdjGR)	1*	81.8	73.3	74.0	67.5	74.1
Total Ammonia Ratio (TAR)	10**	86.2	77.5	80.6	74.0	79.6

692 \* TV- transition value as proposed in Zhang et al (2009);

693 \*\* TV- transition value as proposed in this study

694

695



696

697

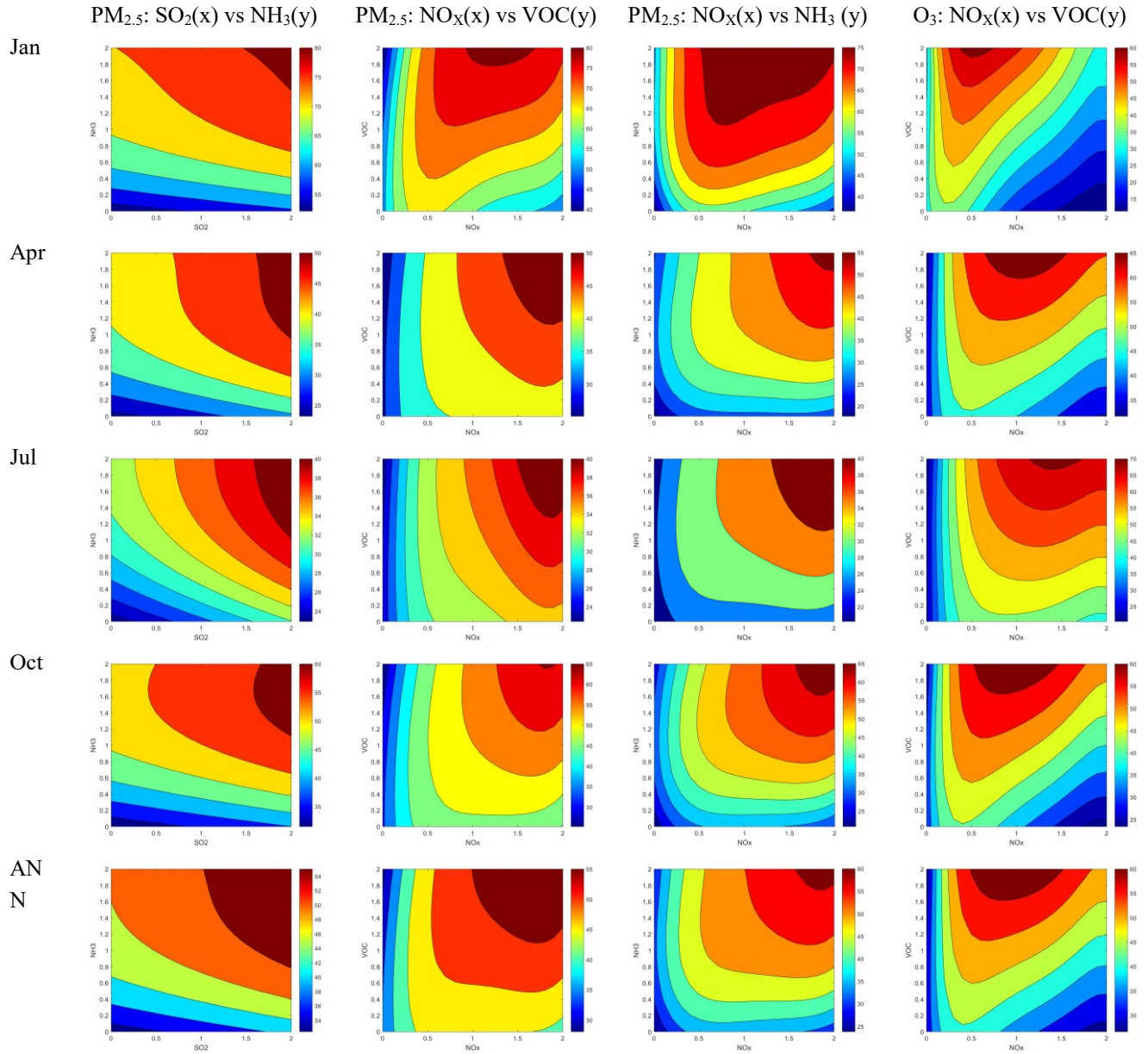
**Figure 1.** Flow of observable response indicator development and application



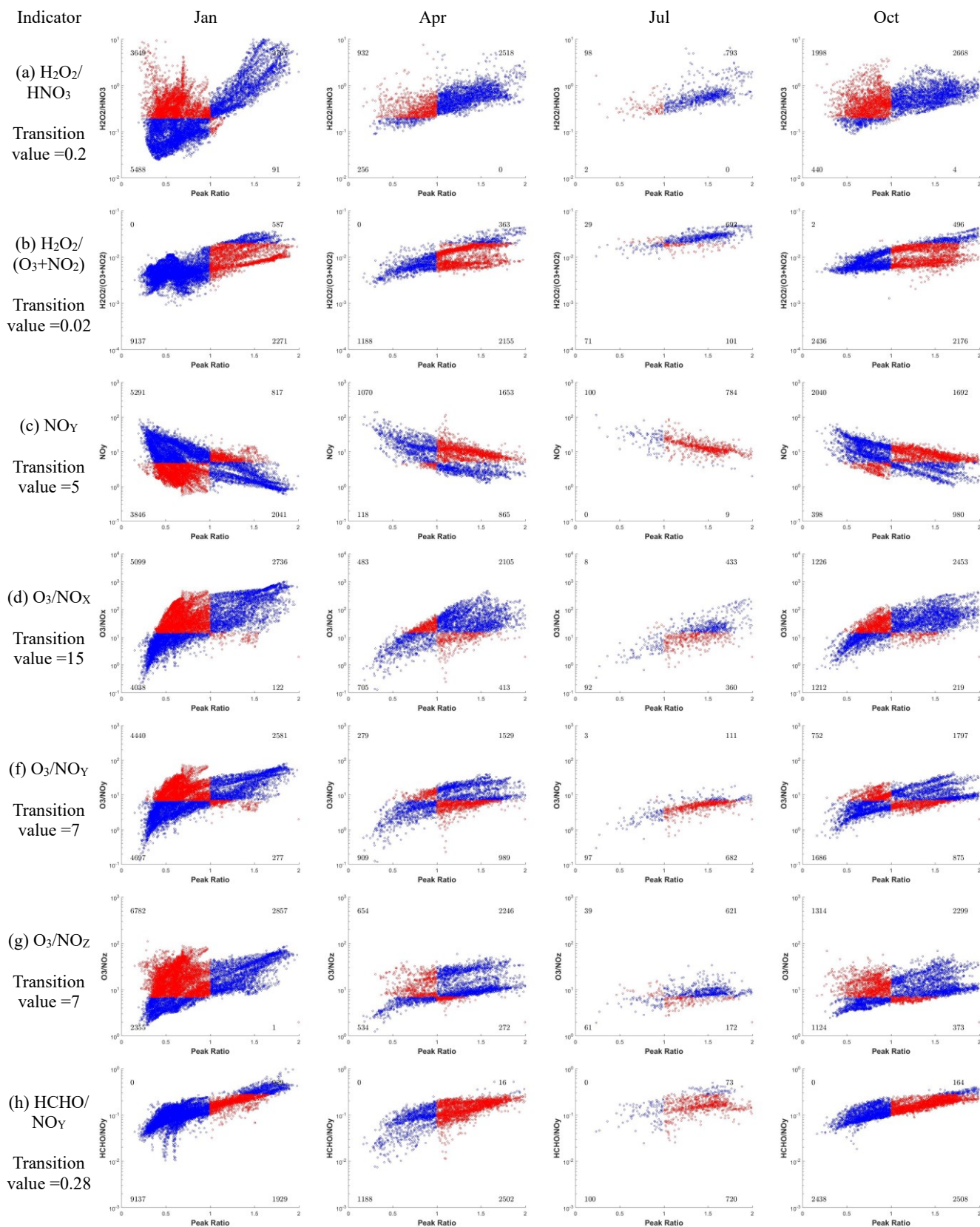
699

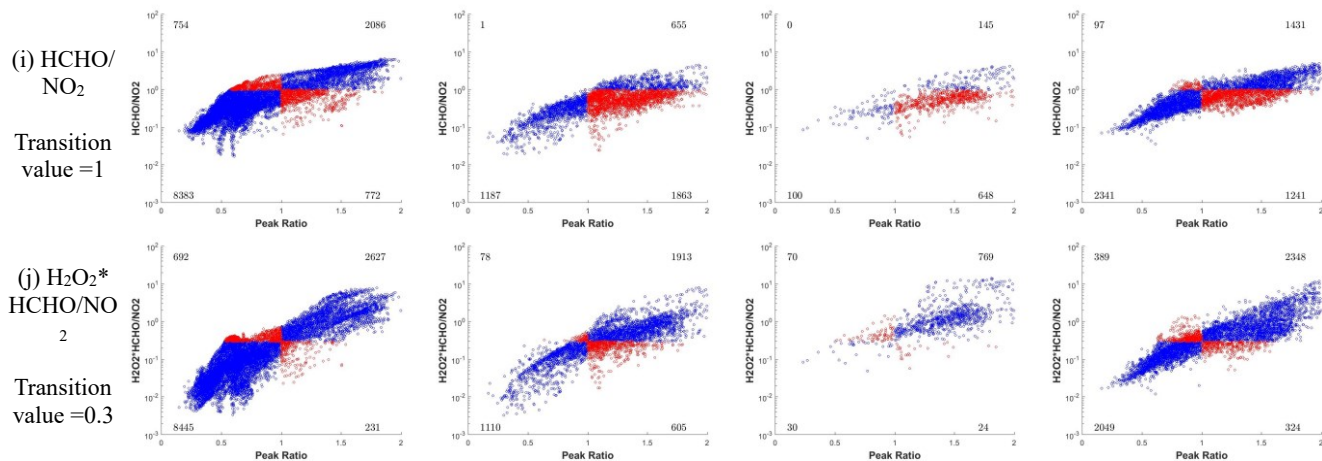
700 **Figure 2.** Simulation domain over mainland China ( $27 \times 27$ -km<sup>2</sup> resolution,  $182 \times 232$  grid cells). The  
 701 31 provinces are BJ-Beijing; TJ-Tianjin; HEB- Hebei; SX-Shanxi; IM-Inner Mongolia; LN- Liaoning;  
 702 JL- Jilin; HLJ-Helongjiang; SH- Shanghai; JS-Jiangsu; ZJ-Zhejiang; AH- Anhui; FJ- Fujian; JX-  
 703 Jiangxi; SD- Shandong; HEN- Henan; HUB-Hubei; HUN- Hunan; GD-Guangdong; GX- Guangxi; HN-  
 704 Hainan; CQ- Chongqing; SC- Sichuan; GZ-Guizhou; YN- Yunnan; TB- Tibet; SHX-Shaanxi; GS-  
 705 Gansu; QH-Qinghai; NX- Ningxia; and XJ-Xinjiang)

706



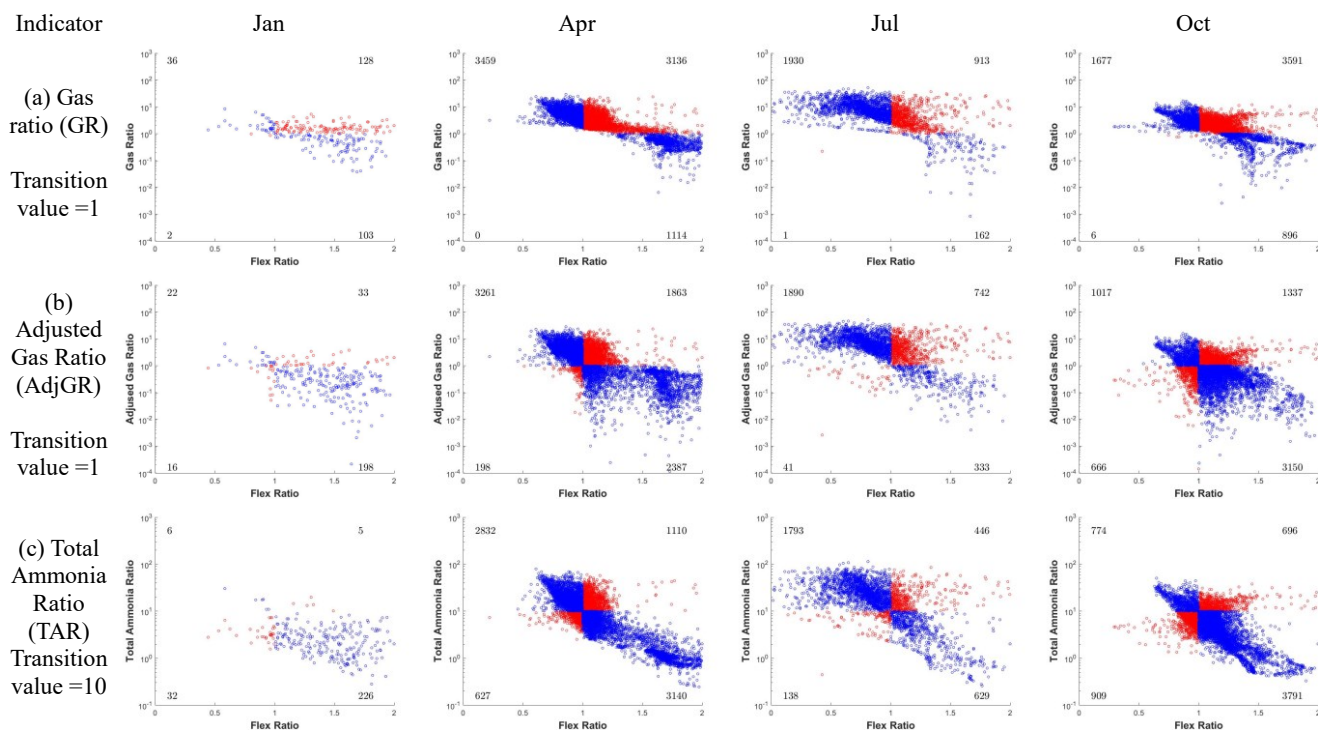
**Figure 3.** Isopleth of population-weighted PM<sub>2.5</sub> and daytime O<sub>3</sub> to precursor emission change in different months. (The x- and y- axes represent precursor emission rates with a baseline of 1, applied to all grid cells in China; background colors represent the population-weighted PM<sub>2.5</sub> and daytime O<sub>3</sub> concentrations in China, with units of  $\mu\text{g m}^{-3}$  for PM<sub>2.5</sub> and ppb for O<sub>3</sub>)



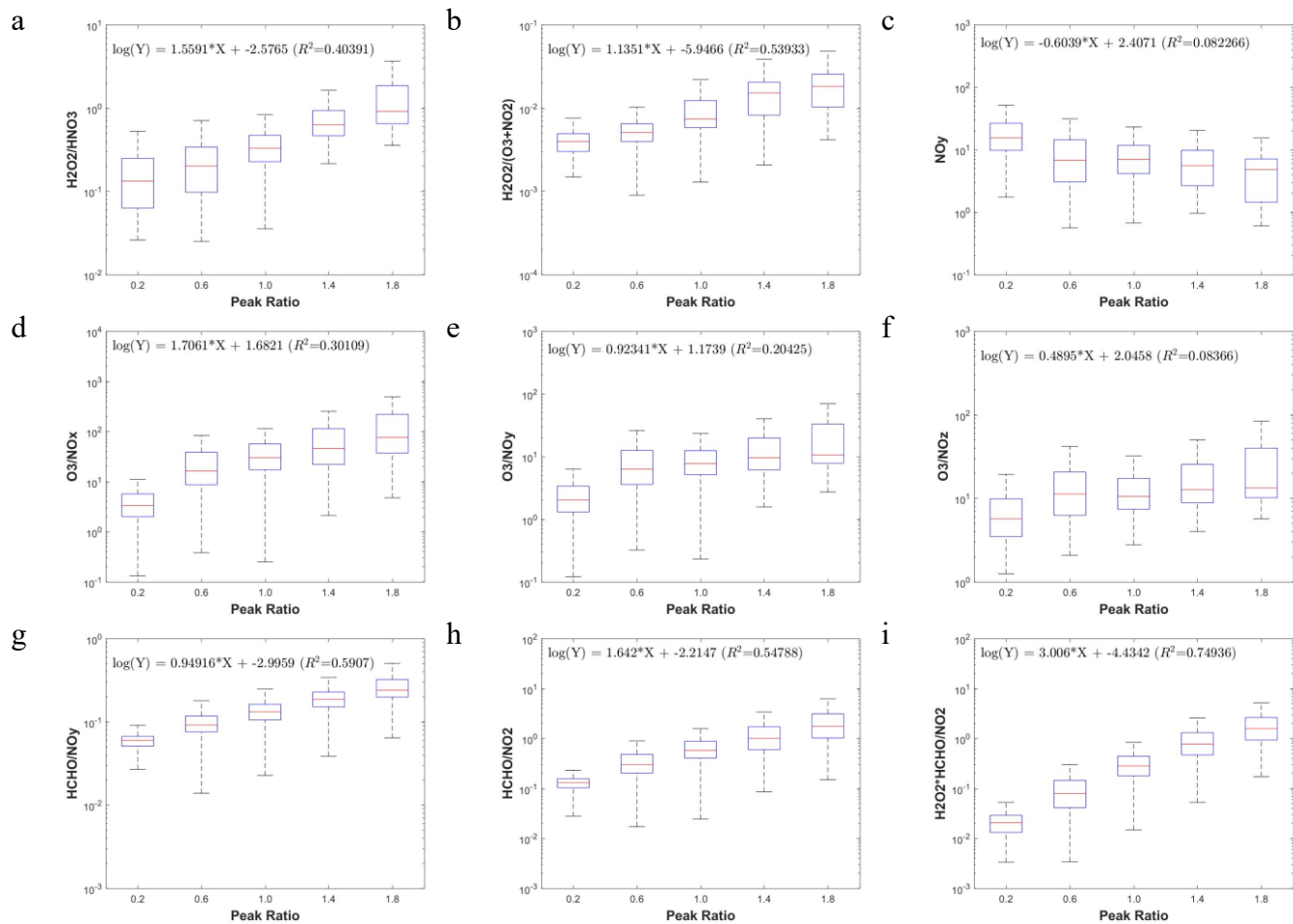


**Figure 4.** Performance of observable indicators in predicting  $\text{O}_3$  chemistry. The x-axis represents the PR values where the transition value is 1, and the y-axis represents the observable indicators. The blue dots represent the grids where  $\text{O}_3$  chemistry is successfully predicted by the observable indicator; the red dots represent the grids where the observable indicator fails to predict  $\text{O}_3$  chemistry. The numbers in the four corners represent the grid number in each section; the number in July is much lower than those in the other months because most grids are located at the  $\text{NO}_x$ -limited regime with  $\text{PR} > 2$  in July.

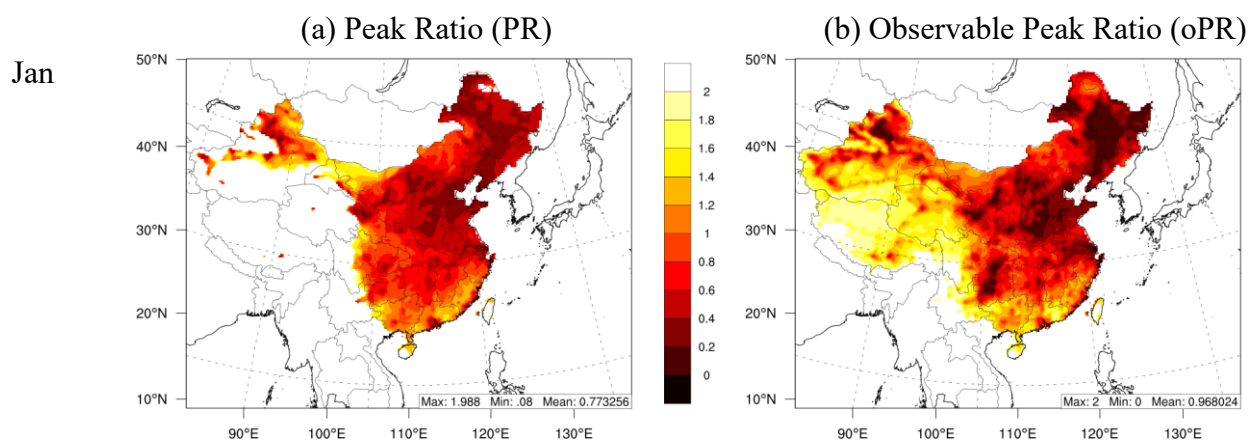


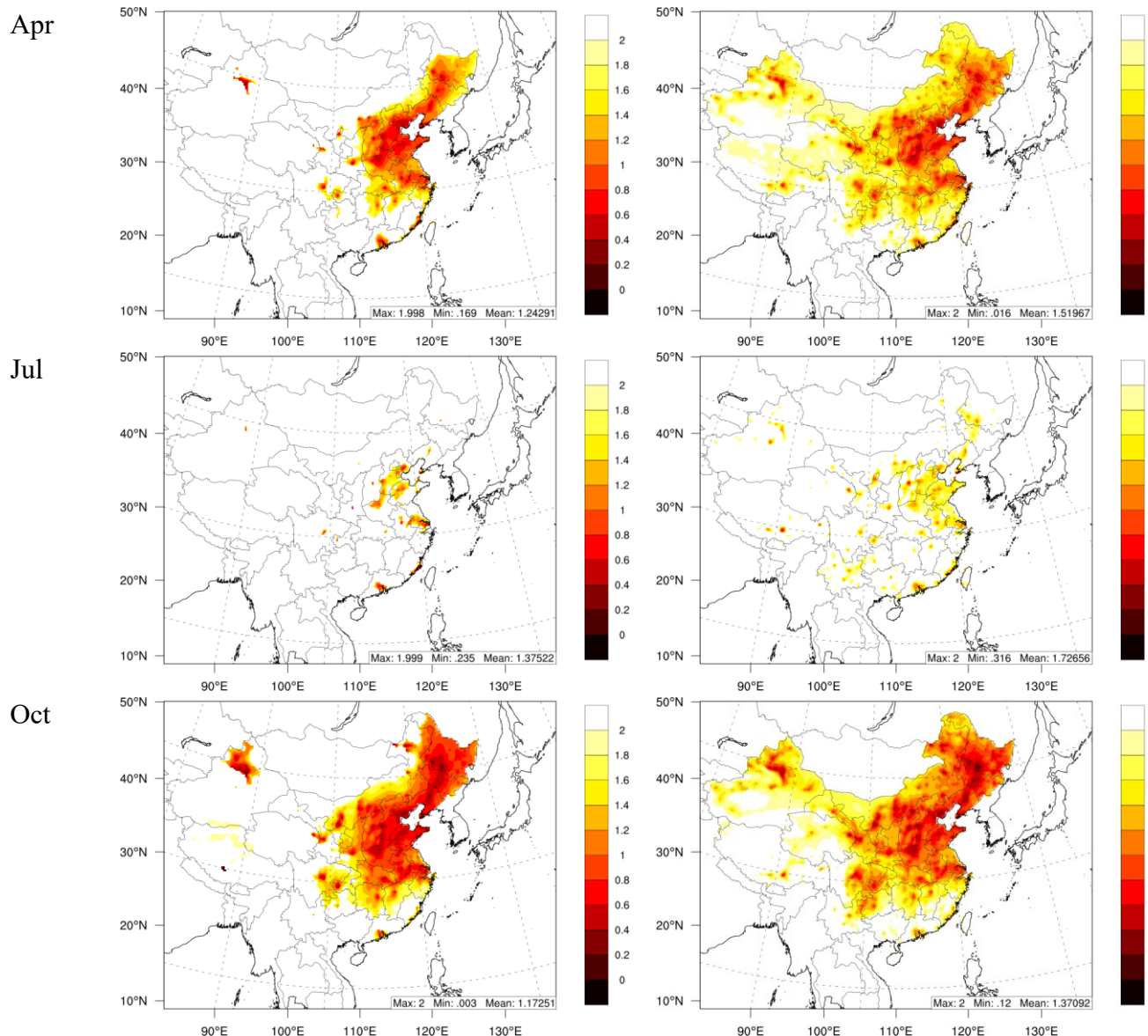


**Figure 5.** Performance of observable indicators in predicting PM<sub>2.5</sub> chemistry. The x-axis represents the FR values where the transition value is 1, and the y-axis represents the observable indicators. The blue dots represent the grids where PM<sub>2.5</sub> chemistry is successfully predicted by the observable indicator; the red dots represent the grids where the observable indicator fails to predict PM<sub>2.5</sub> chemistry. The numbers in the four corners represent the grid number in each section; the number in January is much lower than those in the other months because most grids are located at the NH<sub>3</sub>-poor condition with FR>2 in January.

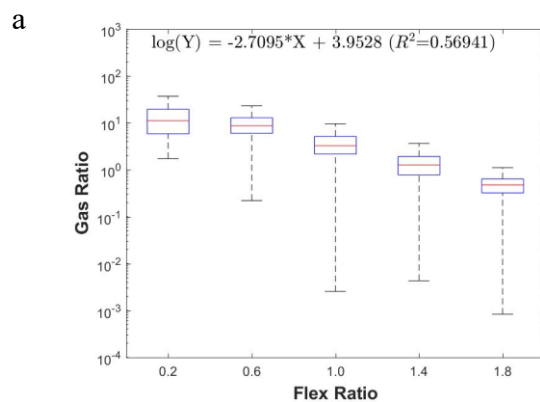


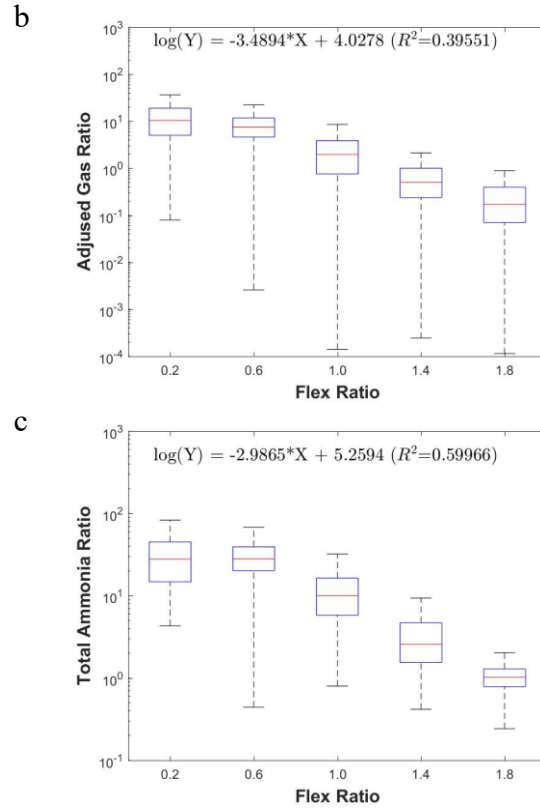
**Figure 6.** Development of observable responsive indicators for  $O_3$  chemistry based on log-linear regressions between observable indicators and the PR.



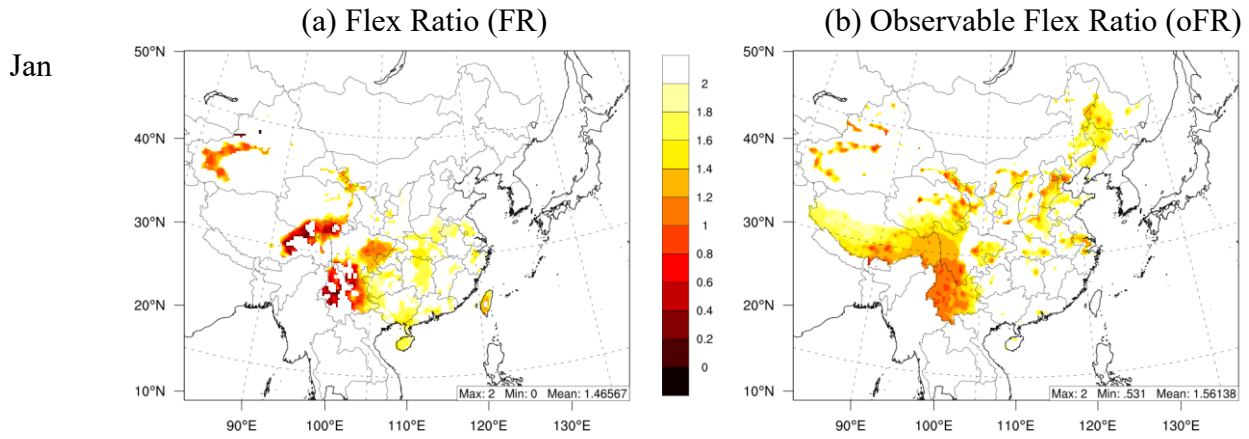


728 **Figure 7.** Comparison of the PR derived from the RSM with that calculated from concentrations for O<sub>3</sub>  
729 chemistry. The oPR was estimated based on H<sub>2</sub>O<sub>2</sub>×HCHO/NO<sub>2</sub>.





**Figure 8.** Development of observable responsive indicators for PM<sub>2.5</sub> chemistry based on log-linear regressions between observable indicators and the FR



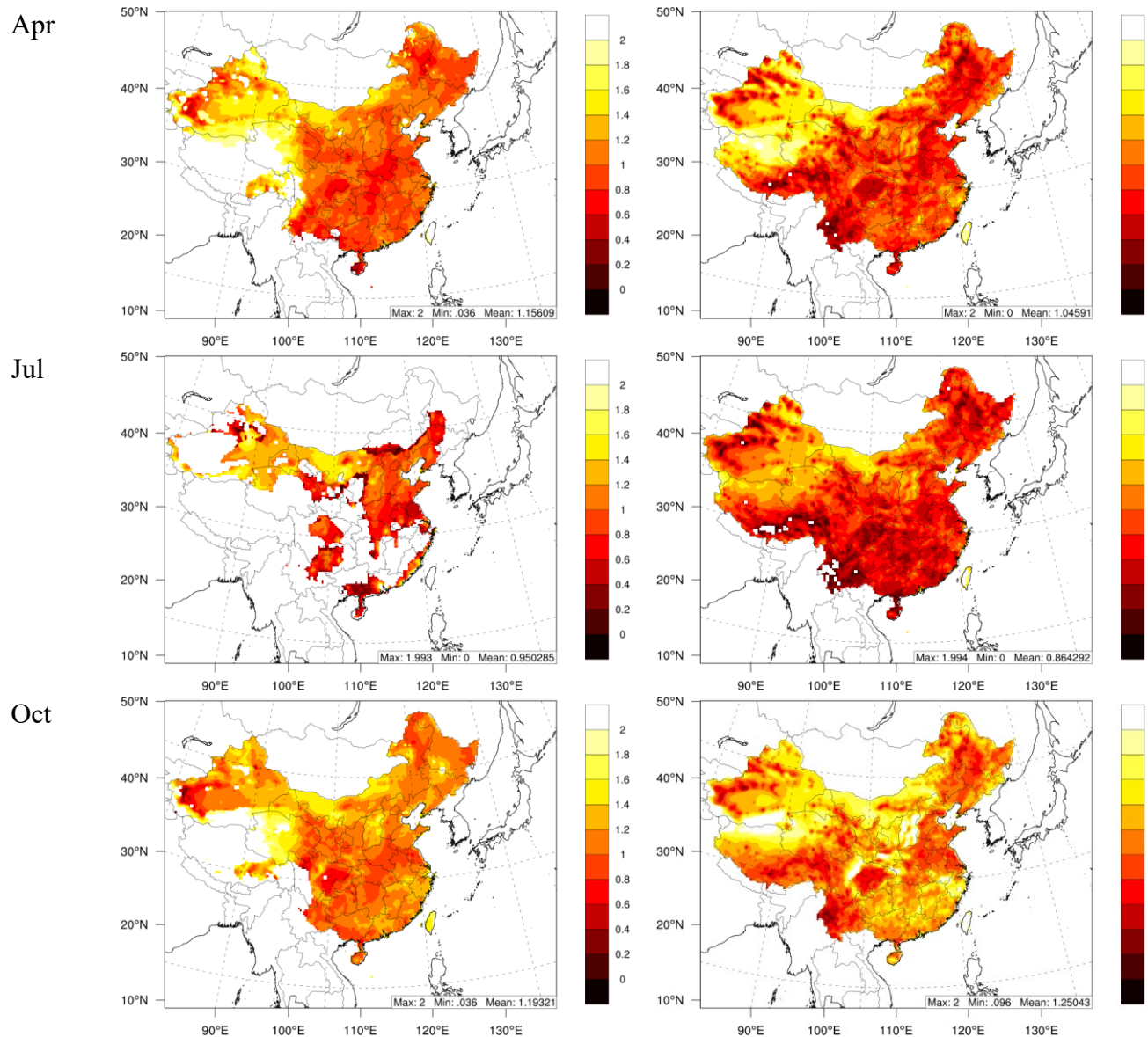


**Figure 9.** Comparison of the FR derived from the RSM with that calculated from concentrations for  $PM_{2.5}$  chemistry. The oPR was estimated based on TAR.

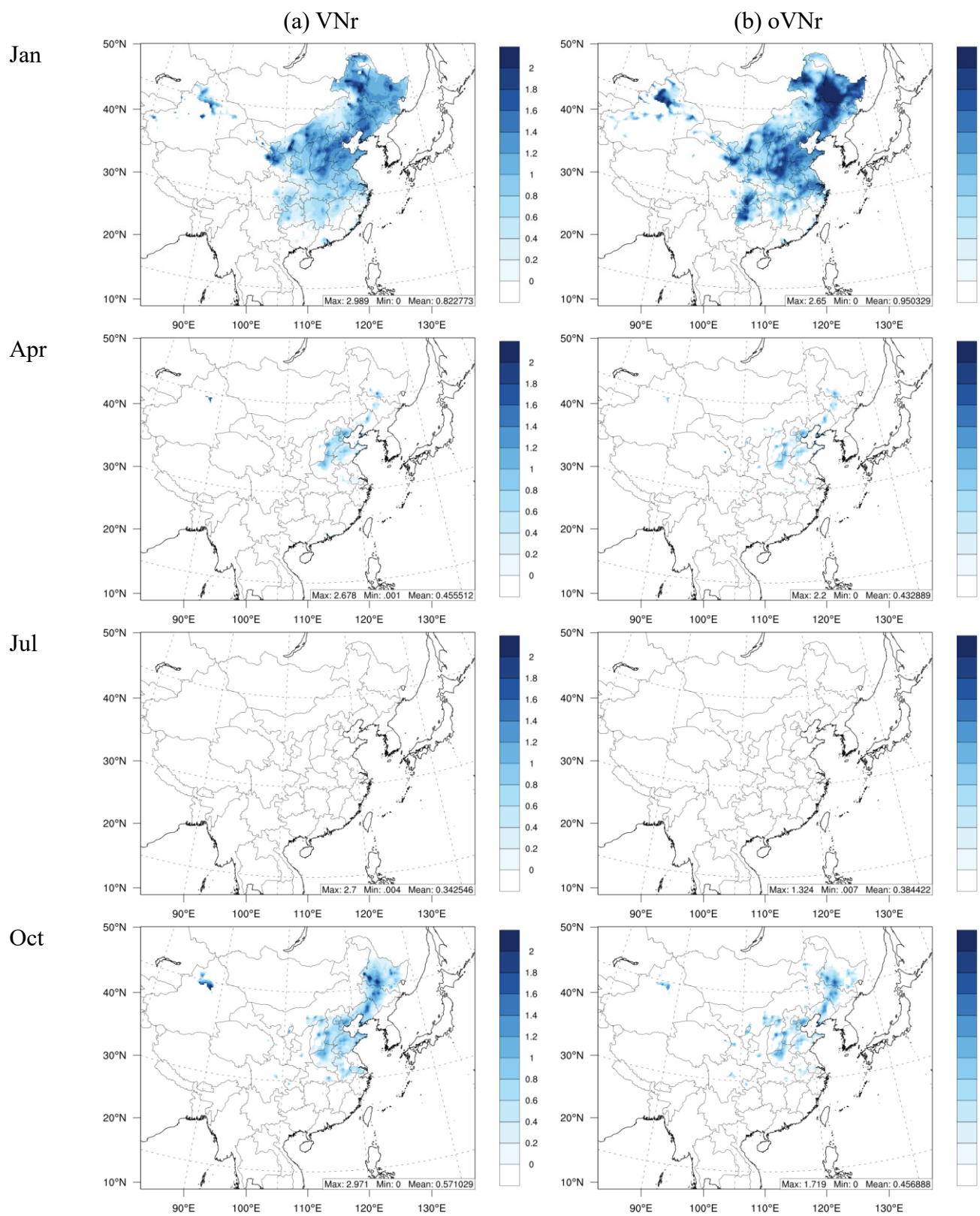


**Figure 10.** Comparison of VNr with oVNr.



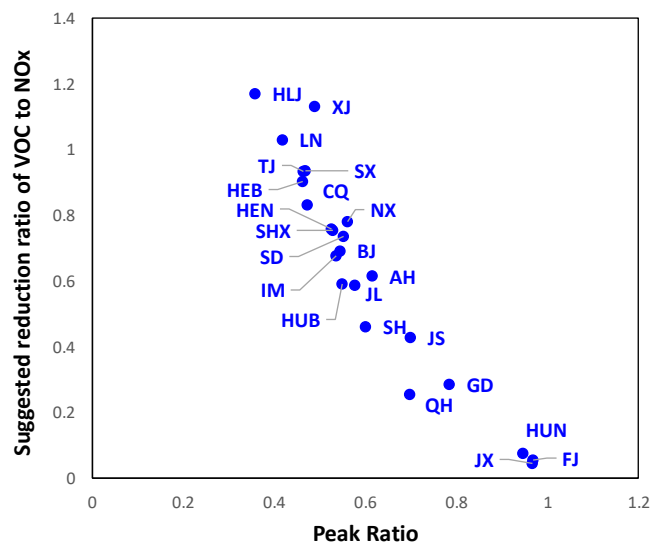


**Figure 11.** Comparison of the annual-averaged PR with VNr in each province in China

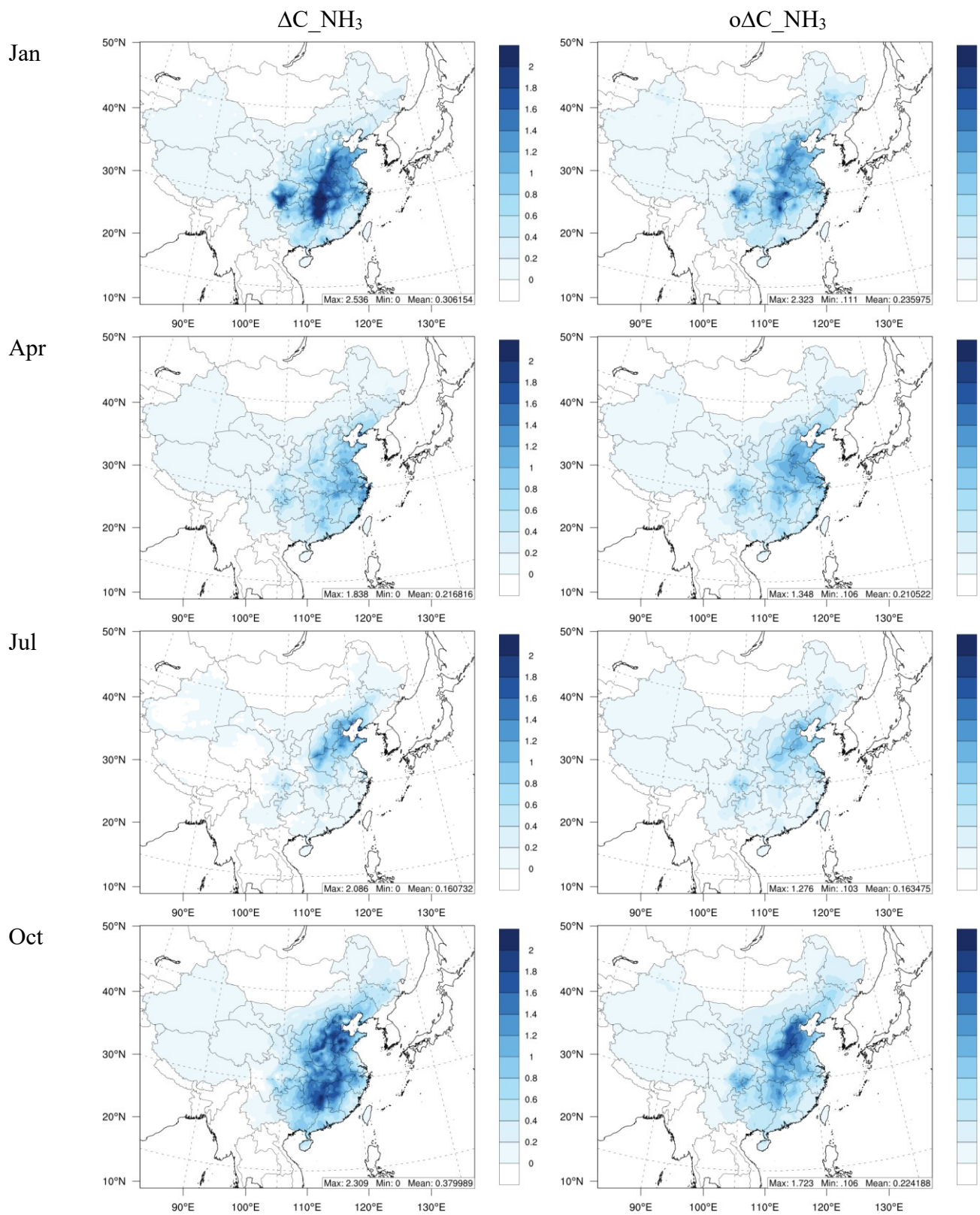


**Figure 12.** Comparison of the benefit in reducing  $PM_{2.5}$  from simultaneous  $NH_3$  reduction ( $\Delta C_{NH_3}$ ) with that calculated from concentrations ( $o\Delta C_{NH_3}$ )



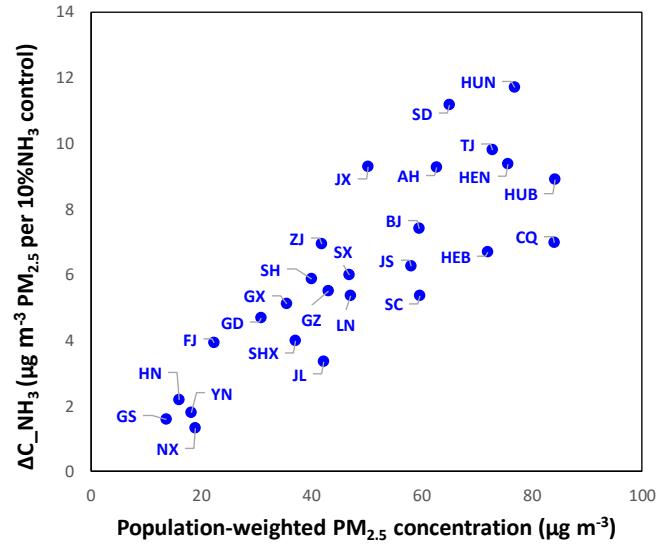


**Figure 13.** Comparison of annual-averaged benefit in reducing PM<sub>2.5</sub> from simultaneous NH<sub>3</sub> reduction ( $\Delta C_{NH_3}$ ) and population-weighted PM<sub>2.5</sub> concentration in each province in China

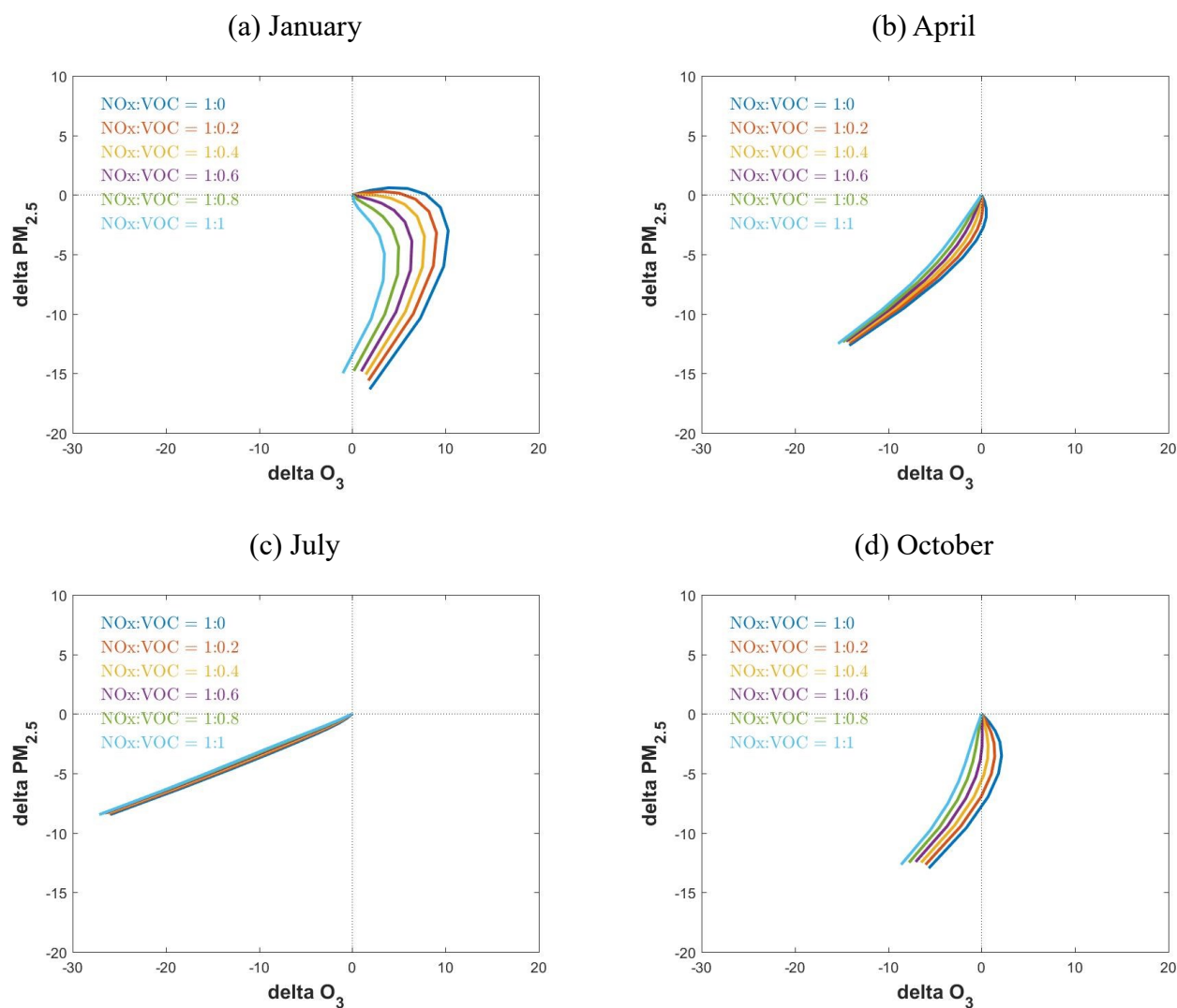


**Figure 14.** Control effectiveness with different  $\text{NO}_x$  and VOC ratios in reducing population-weighted  $\text{PM}_{2.5}$  and  $\text{O}_3$  concentrations (in  $\mu\text{g m}^{-3}$ ) in China ( $\text{NO}_x$  is from no control to 80 % reduction)